IN-PLANE CYCLIC SHEAR PERFORMANCE OF PIPE STEM

REINFORCED COB WALL

A Thesis

presented to

the Faculty of California Polytechnic State University,

San Luis Obispo

In Partial Fulfillment

of the Requirements for the Degree

Master of Science in Civil and Environmental Engineering

by

Dezire Q'anna Perez Barbante

December 2019

COMMITTEE MEMBERSHIP

TITLE: In-Plane Cyclic Shear Performance of
Pipe Stem Reinforced Cob Wall

AUTHOR: Dezire Q'anna Perez-Barbante

DATE SUBMITTED: June 2019

COMMITTEE CHAIR: Daniel C. Jansen, Ph.D., PE
Professor of Civil and Environmental Engineering

COMMITTEE MEMBER: Bing Qu, Ph.D., PE
Associate Professor of Civil and Environmental
Engineering

COMMITTEE MEMBER: Anthony Dente, PE
Principal of Verdant Structural Engineers

ABSTRACT
In-Plane Cyclic Shear Performance of Pipe Stem Reinforced Cob Wall
Dezire Q'anna Perez-Barbante

This thesis investigates full-scale pipe stem reinforced cob walls under in-plane cyclic shear loads. Cob is the combination of clay subsoils, sand, straw and water that is built in lifts to produce monolithic walls. There is insufficient amount of information on cob as a building material in today's age. The prior research that exists has examined varying straw content and type, water content, and mixture ratios to determine their effect on strength. There is currently one report that analyzes full-scale cob walls under in-plane loading. This thesis looks to iterate the full-scale tests and specifically studies the effect of reinforcement on cob walls. Concurrent to this research, another thesis was written that investigates a full-scale wire mesh reinforced cob wall under in-plane cyclic shear loads.

From the data collected, a shear failure was suggested for the stem pipe wall. There appeared to be a large amount of ductility from the data and the cracks formed. Ductility, a seismic response modification factor (R-Factor) and stiffness were calculated using the yield point and ultimate loads. Iterations of this research and those performed in the past can be helpful in integrating cob into the California Building Code.

Keywords: Earthen Building Material, Cob, In-Plane Shear, Furthest Point Yield Method, Ductility, Seismic Response Modification Factor, R-Factor, Stiffness

ACKNOWLEDGMENTS

TABLE OF CONTENTS

LIST OF TABLES

LIST OF FIGURES

1.   INTRODUCTION

1.1.   Background

Earthen construction has been utilized by man beginning approximately 10,000 years

ago. These buildings have been viewed as models for "green" practice and their methods are

coming full circle and being re-learned. It is estimated today that about one-third to one-half of

the world's population still live and/or work in earth dwellings. Earthen construction is used

throughout the world, due to its versatility and accessibility. Adobe, sod, rammed earth, straw-

clay, and wattle-and-daub are some of the many earthen construction techniques that have

been used to date.

"British Cob" was one of the first methods of its kind. Cob is the combination of clay

subsoils, sand, straw and water that are formed into monolithic walls. The materials for cob are

mixed together by stomping (or machinery, if the resources are available) either on a tarp or in a

pit depending on the amount of cob being produced. The British Cob is then molded and

leveled, with the use of a paddle, into the walls in lifts ranging from 6 inches to 3 feet in height.

Each lift is left to dry for 2 weeks before an additional lift is threaded into the previous layer to

create a complete connection. The final product includes walls with thicknesses ranging from 20

to 36 inches and heights as large as 23 feet. Cob houses in England date as far back as the 13th

century and can last about 100 years before needing repairs.

Long neglected cob homes in England needed repairs, resulting in British Cob being

reintroduced. The reemergence of British Cob has sparked interest in the United States, with

interest led by the Cob Cottage Company in Western Oregon. Due to their lack of knowledge

with the material, construction techniques differ enough from British Cob to warrant a different

name: "Oregon Cob". Oregon cob utilizes the same materials as British Cob but puts more

emphasis on obtaining the proper ratio of materials. Focusing on the proper ratio has led to

higher strengths and more stable structures. Paddles that are used on British Cob to shape and level walls are replaced with trimming techniques, where walls are built larger than necessary and trimmed to their desired dimensions. The excess cob can then be reused in the next mixture. Oregon Cob also promotes the use of loaves to transport cob farther distances and to higher lifts with ease.

The most crucial obstacle to overcome when utilizing cob as a building material is not the material or the techniques themselves, but the perspective from modern society and their understanding of the construction process in a new, alternative way (Snell and Callahan, 2009). Earth as a building material was previously viewed as a product of poverty and fell out of use. The use of earth did not diminish because of its lack of durability, but because it was not deemed socially acceptable. The modern housing industry contributes to 50% of all pollution in the world, with cement processing alone creating 8% of total greenhouse gases. The planet's ecology continues to suffer from the industrial revolution and technological age. People need to take conscious steps on a personal level to aid the planet, which can begin by addressing the house they live in (Weismann and Bryce, 2006).

Cob is not always the best solution, as there are many factors that must be considered prior to working with cob. The construction of all buildings depend on their location and the climate, especially earthen construction. A main ingredient in cob, is a clay subsoil, where the perfect clay is not always easily accessible. If the clay consists of too much silt particles, the structural integrity of the cob is at risk. The clay mixture needs to contain a good amount of gravel and sand, which can always be added to a clay, if necessary. Clay is also unstable in the sense that it shrinks when it is too dry, causing neighboring particles to be sucked closely together. On the other hand, when clay is too wet, it can swell, soften, or erode completely, affecting the structural stability of the cob. The excess water in cob also has the potential to

2

freeze which can expand and crumble the cob again altering the structural integrity. Besides location's effect on cob, another setback to consider is the time needed to allow cob to dry to reach an ideal strength. When there is moisture in the air, cob can take longer to reach its proper strength, therefore, extending the construction time, and ultimately increasing construction costs.

Aside from these setbacks, there are many benefits in cob construction. The materials needed to make cob cost little to nothing. Many development sites excavate sand and clay subsoils and must pay to ship the excess material off site; they might even be willing to give it away for free to save themselves transportation expenses. Cob can also be mixed without the use of heavy machinery, resulting in lower construction costs. When the lifts are connected properly, cob is built as a monolithic unit, and therefore has no joint weak points. Due to its high density, thermal temperatures transfer slowly through cob walls which allows cob buildings to maintain a constant interior temperature. Finally, cob is ecologically friendly; there are no risks of off-gassing or contaminating its surroundings. The materials for cob are taken from the earth and can easily be put back when done.

1.2. Objective

Currently, cob revival is in its infancy and there are no specific codes or standards due to the lack of information on the material. The Cob Research Institute is hoping to legalize the construction of cob by developing safe and easily understood standards. The first step necessary is to investigate cob as a building material in areas prone to earthquakes. This research focused on determining material properties of cob and the behavior of full-scale cob walls with varying reinforcement under in-plane cyclic loading. This paper specifically discusses the modulus of rupture of cob and the behavior of a full-scale hybrid cob wall with steel pipe reinforcing ("pipe stem wall") under in-plane cyclic loading. Another paper, by Julia Sargent, produced at the same

time as this paper, discusses the compressive strength of cob and the behavior of a full-scale hybrid cob wall with reinforcing mesh under in-plane cyclic loading. To study this, a portable loading frame was constructed to apply the in-plane cyclic loading and a data acquisition system was set up to analyze the displacement due to loading to determine shear or bending failure. This research was conducted to gain a better understanding of cob as a building material and determine respective seismic response modification factors, R factors, of the pipe stem wall.

1.3.   Contents and Layout

This thesis evaluates the relevant background, design, methods, results, analysis, and conclusions of these experiments. It is divided into the following eight chapters:

- Chapter 1 provides background information on cob and discusses the primary research objectives of this research.

- Chapter 2 investigates the prior research performed on cob, including material properties with varying material types and ratios, and maximum stresses found from different loading methods.

- Chapter 3 inspects the wall components in this research, both raw and composite materials. This includes a description of the mixing process and the testing procedures followed to determine material properties. These established material properties are compared to the values concluded in prior research.

- Chapter 4 reports the construction process executed to erect the pipe stem wall.

- Chapter 5 reviews the design process for the portable loading frame, including calculations, frame materials, and the construction process of the frame itself.

- Chapter 6 describes the testing setup, containing the data acquisition system, and the procedure followed, including the implemented displacements. This chapter also introduces the raw data collected during the test.

- Chapter 7 analyzes the results from the test, specifically the yielding and ultimate stresses and displacements. These values are used to determine the ductility, over strength factor, and the R factor.

- Chapter 8 recaps the key concepts from this report and recommends future research to follow these tests.

2.   LITERATURE REVIEW

2.1.   Effect of Straw Length and Quantity on Mechanical Properties of Cob (Rizza & Böttger, 2013)

The purpose of this study was to analyze the reinforcement contribution to cob from natural fibers, similar to steel in concrete. The straw in cob provides ductility to the material which allows visual warning signs if the structure is ever compromised. The method for testing the reinforcement in cob consisted of testing blocks of cob with varying mixtures and different straw types (long vs chopped straw). In addition to the extra straw, sand was removed from the mix because the fiber replaces the need for it. The soil used in these blocks was classified with a medium-to-high range of plasticity.

Compressive strengths were determined by compressing rectangular prisms through their longest lengths. Failure occurred due to shear as opposed to pure compression, as seen in Figure 2.1. This failure mode could be due to the eccentricity of the specimen formed from the specimen drying into trapezoids. Flexural strength tests were conducted following a single-point compression centered on the beam. Finally, tensile strengths were found applying "line loads along the length of the cylinder" (Rizza & Böttger, 2013), which can be viewed in Figure 2.2.

Figure 2.1: Compressive Strength Failure   Figure 2.2: Tensile Strength Tests

The conventional cob resulted in larger compressive strengths than both the mixes

containing long straw and chopped straw. The stress-strain curves created from these tests can

be seen in Figure 2.3. The conventional cob also had a higher Young's Modulus than the others.

The chopped straw specimen obtained the highest flexural strength from the Modulus of

Rupture test, however the greater ductility was observed in the long straw mixture. In

conclusion, chopped straw and long straw specimens resulted in larger ductility than

conventional cob, but their compressive strengths were much lower. This could potentially be

due to excessive cob not allowing a strong bond to form with the clay subsoil. A summary of the

results from this test can be seen in Table 2.1.
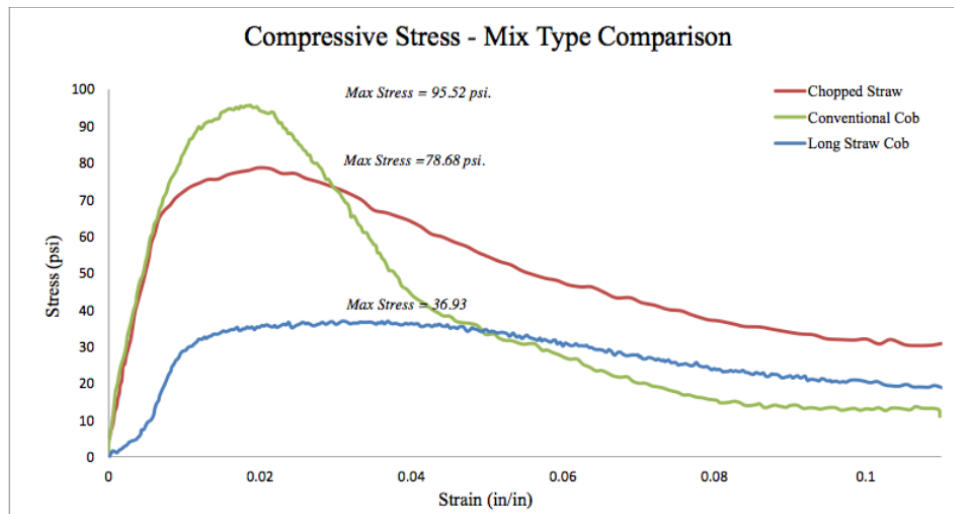
Figure 2.3: Compression Test Results

Table 2.1: Results from Rizza & Böttger, 2013

RIZZA AND BÖTTGER, 2013						
Mixture	Moist Unit Weight (lb/ft^3)	Straw Content by Volume (%)	Compressive Strengths (psi)	Modulus of Elasticity (psi)	Modulus of Rupture (psi)	Tensile Strengths (psi)
Conventional	92.5	18.7	95.52	10,371	77.56	26.14
Chopped Straw	65.0	47.9	78.68	9,414	141.74	15.91
Long Straw	60.5	41.5	36.93	5,405	115.39	16.52

2.2. Index and Engineering Properties of Oregon Cob (Pullen & Scholz, 2011)

The purpose of this research was to test the different mixing methods of cob from five experienced builders. Six mixtures were used, with one builder providing two mixtures only differing in straw length. Each builder also provided the constituent materials for their mixtures, so their properties could be determined. The six mixtures varied in sand, soil, and straw type explained in Table 2.2. This research analyzed several different properties: soil plasticity (ASTM D4318), sand gradation (ASTM C136) and void content (ASTM C1252), straw length and tensile strength, and mixture water content (ASTM C566), shrinkage, unit weight (ASTM C138), compressive strength, modulus of rupture and modulus of elasticity. The mixture properties were determined following the test methods used for concrete.

Table 2.2: Six Mixture Types

| Mixture | Soil | Sand | | Fiber |
	Source	Product Name	Visual Angularity	Description
A	Philomath	Coarse Washed River Sand	Semi-rounded	Hand-cut field hay
B	Philomath	Coarse Washed River Sand	Semi-rounded	Hand-cut field hay
C	Estacada	Sharp Concrete Sand	Semi-rounded	Baled oat straw
D	East Portland	Mason Sand	Angular	Bedding straw
E	East Portland	Plaster Sand, Multi-Purpose Sand	Semi-angular	Baled straw
F	Corvallis	River Sand	Semi-rounded	Baled oat straw

The compressive strength test and the modulus of rupture tests were performed following ASTM C39 and ASTM C78, respectively, with a few modifications. Examine the test setups in Figure 2.4. These test utilized cylindrical and rectangular blocks of cob, however, they were created with more lifts and consolidation by hand to replicate the actual construction in the field. A summary table of the results can be seen in Table 2.3.
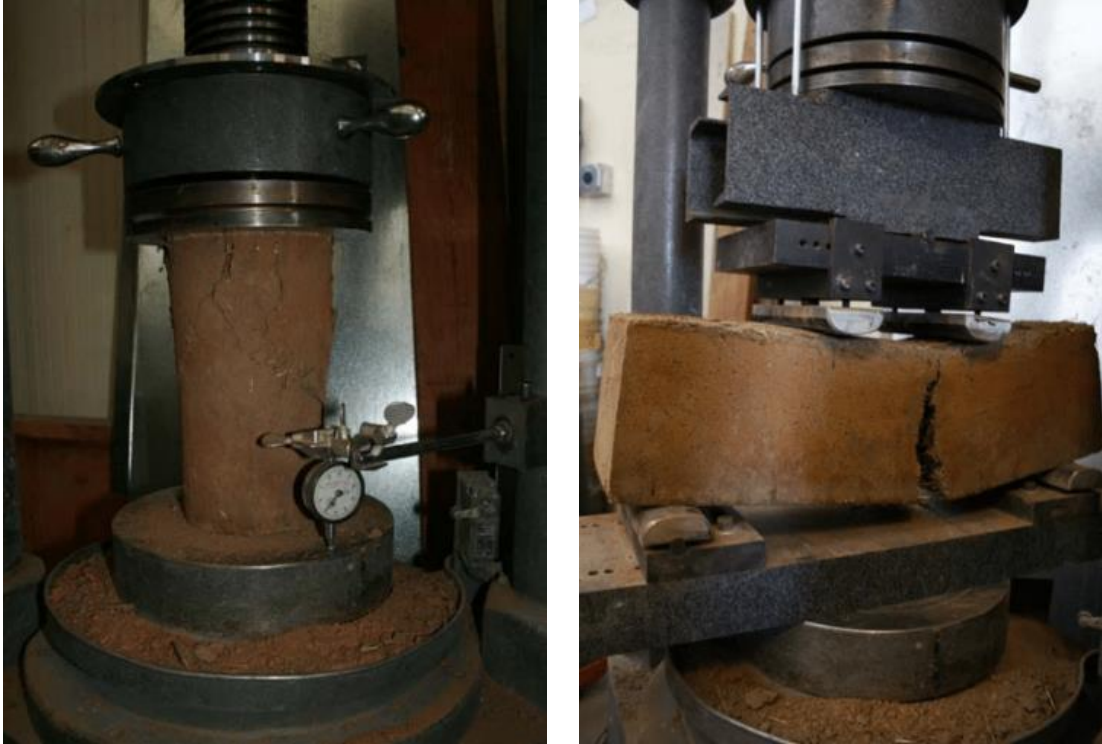
Figure 2.4: a) Compression Test Setup b) Modulus of Rupture Test Setup

Table 2.3: Summary of Results

Mixture	Moist Unit Weight (lb/ft³)	Dry Unit Weight (lb/ft³)	Water Content (%)	Compressive Strength (psi)	Modulus of Rupture (psi)	Tensile Strengths (psi)	Modulus of Elasticity (psi)
A	117.0	92.7	26.2	102	34.6	2,400	1,600
B	118.2	93.8	26.0	107	31.5	2,600	2,000
C	122.0	99.2	23.0	90.4	23.5	700	2,100
D	118.6	95.0	24.9	65.1	10.8	1,900	43,000
E	123.0	103.7	18.7	119	23.6	1,100	10,000
F	116.2	93.9	23.8	129	26.2	500	4,700
Average	119.2	96.4	23.8	102	25.0	1,500	11,000
Std. Dev.	2.74	4.24	2.8	22.5	8.3	890	16,000

The above table title row reads: PULLEN AND SCHOLZ, 2011

The vertical shrinkage appeared to be less than the horizontal shrinkage which could be due to the compaction in the vertical layers. Regarding the reinforcement, the fibers need to be at least six inches long to develop an adequate bond. Also, it was observed that the use of hay resulted in a higher tensile strength than those produced with straw. Referencing the sand

content, it appeared that an increase in sand content resulted in a decrease in shrinkage and an increase in compressive strengths.

2.3.   The Performance of Cob as a Building Material (Saxton, 1995)

The purpose of this research was to determine an optimum straw content to include in a cob mixture. This was established by testing cob mixtures with different straw and moisture contents for the following: ease of mixing, suitability for placing, rate of drying, shrinkage, compressive strength, deformation, and weathering. The different mixtures are defined in Table 2.4 and can be viewed in Figure 2.5.

Table 2.4: Defined Mixtures

Straw content (% by weight)	Moisture content					
	Slightly dry		About right (Optimum)		Slightly wet	
0	1A	1B	7A	7B	6A	6B
0.2	2A	2B	8A	8B	3A	3B
0.6	4A	4B	9A	9B	5A	5B
1.2			10A	10B		
2			11A	11B		
3			12A	12B		
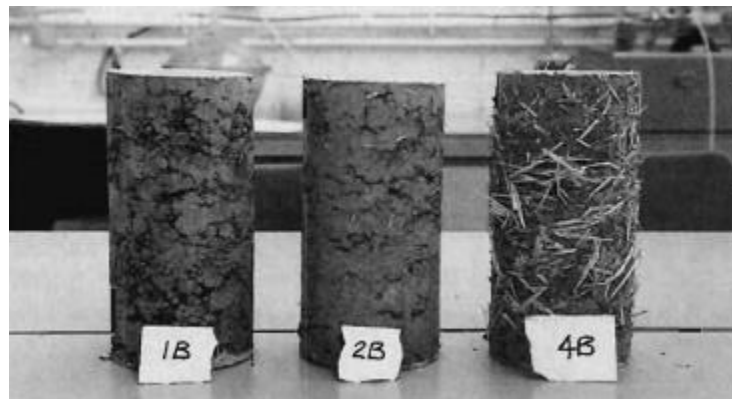
Figure 2.5: Varied Cob Specimen

It was concluded that the increase in straw content forced an increase in water content to maintain a suitable mix. These increased components resulted in the most shrinkage but smaller shrinkage cracks formed. The increase in straw content also resulted in larger strengths

and larger strains at failure. Optimal straw content was found to be between 1% and 1.5% and the moisture content was found to be about 9% resulting in zero shrinkage and strengths around 600 kN/m^2.

2.4.   Mechanical Behavior of Earthen Materials: a Comparison between Earth Block Masonry, Rammed Earth and Cob (Miccooli, Müller, & Fontana, 2014)

The purpose of this research was to determine material properties of cob in comparison to other earthen building methods. This was done by testing three different methods to determine compressive strengths, tensile strengths, Young's modulus, strains, and shear properties. The cob mixture for these tests consisted of 18% gravel and sand, 61% silt, and 21% clay. The cob samples for material property tests were created by cutting out smaller pieces from a larger specimen, preserving the original orientation of the cob.

The compression tests were performed until failure was reached, and LVDTs were arranged both parallel and perpendicular to the loading direction to record deformations. As seen in Figure 2.6, cob exhibits lower compressive strengths compared to rammed earth and earth block masonry but displays larger displacements, resulting in higher ductility.
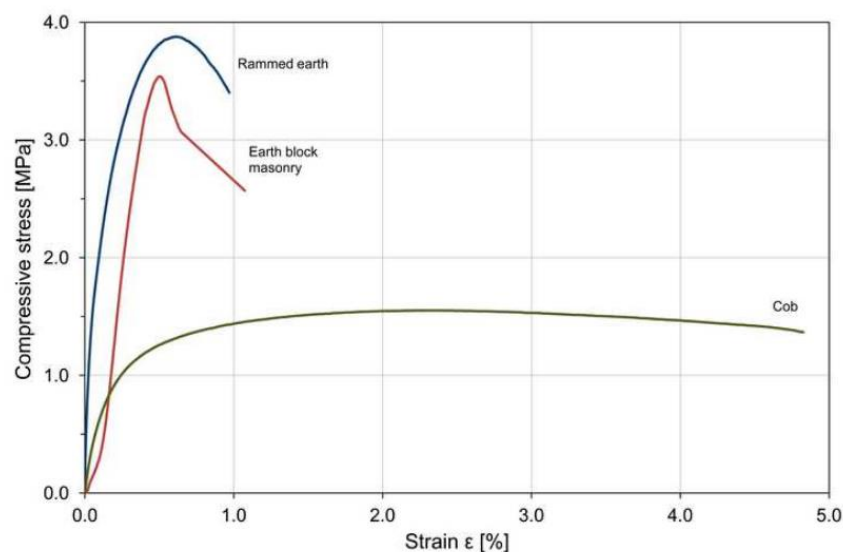
Figure 2.6: Compressive Strength Test Results

11

To establish shear strengths in the materials, a diagonal compression test was performed; see Figure 2.7. This procedure utilizes full-scale walls to be tested, therefore monolithic walls were created for cob, following typical construction procedures of a cob wall. Evaluating Figure 2.8, the cob specimen performed better than in the compressive strength tests relative to the other earthen construction techniques. This test resulted in shear strengths larger than earth block masonry, and slightly less than rammed earth. Again, the ductility of cob can be observed from the large strain values. The higher ductility provides buildings the ability to deform substantially before collapsing which is a key factor in saving human lives and foreseeing necessary repairs before it is too late. Table 2.5 summarizes the information from this research, as well as the prior research used for comparison.
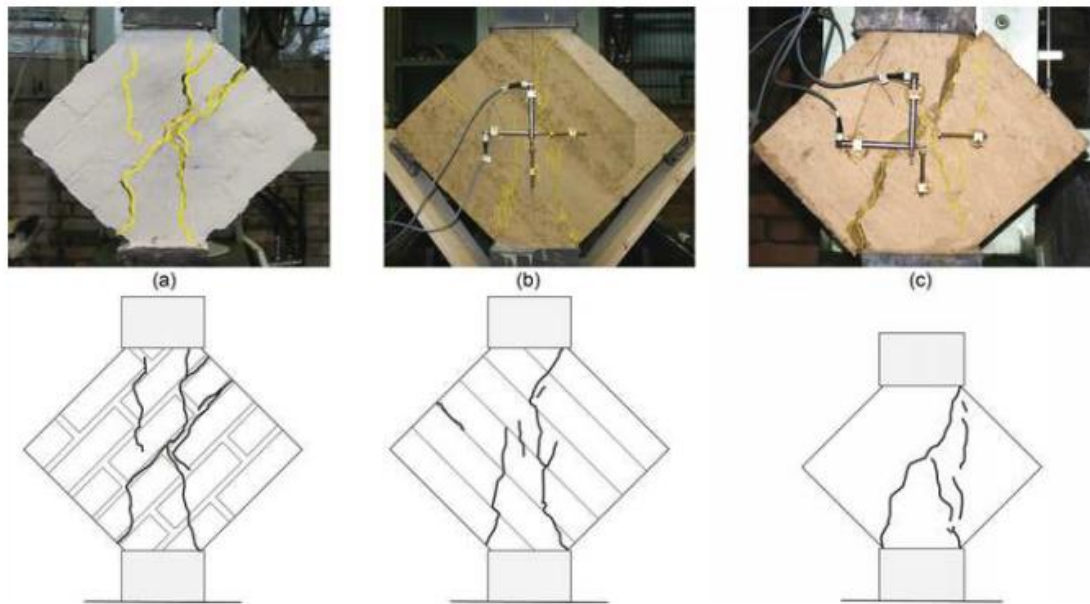
Figure 2.7: Diagonal Compression Tests
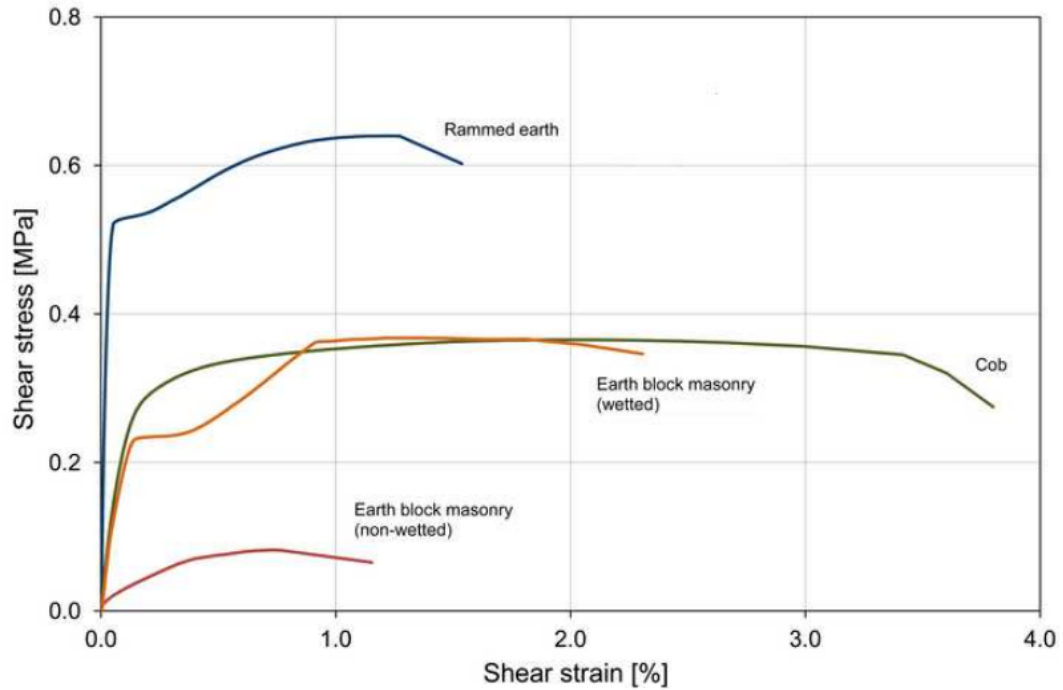
Figure 2.8: Shear Strength Test Results

Table 2.5: Summary of Results from Miccooli, Müller, & Fontana, 2014

MICCOLI, et al., 2014						
Sample	Bulk Density (kg/m³)	Compressive Strength (Mpa)	Tensile Strength (Mpa)	Modulus of Elasticity (Mpa)	Poisson's Ratio	Vertical Strain (%)
ZIEGERT, 2003	1400-1700	0.45-140	0.09-0.34	170-335	-	-
MICCOLI, et al., 2014	1475	1.59	0.50	651	0.15	0.123

2.5.   Cob Property Analysis (Brunello, Espinoza, & Golitz, 2018)

The purpose of this research was to determine material properties for cob and perform the first full-scale wall tests under in-plane lateral cyclic loads. Four walls were constructed with varying levels of reinforcement and height to length ratios. The constituent materials and cob samples were tested for material properties, and the full-scale walls were tested to determine R factors.

The cob samples underwent modulus of rupture, compressive strength, and modulus of elasticity tests. The modulus of rupture tests were performed in double-point compression. The flexural strength was calculated to be 54.4 psi, which seems lower in comparison to concrete.

13

This could be due to the smaller length of the straw used in the mixture. The compressive tests executed were testing the change in compressive strengths due to the specimen's drying period. There appeared to be a linear relationship between compressive strength and drying time, resulting in a 7.33 psi strength increase per month of drying time. Modulus of elasticity was found by stretching cob columns and recording the elongation of the specimen. Table 2.6 compiles the material properties found for the cob mixture.

Figure 2.9: a) Modulus of Rupture Test Setup b) Compression Test Setup

Table 2.6: Summary of Cob Material Properties

BRUNELLO, et al., 2018				
Sample	Flexural Capacity (psi)	Compressive Strength (psi)		
		1 Month	2 Months	3 Months
T1	60.4	92	115	138
T2	56.3	100	85	118
T3	46.5	121	109	122
Average	54.4	104	112	126

2.6.   Cob: A Sustainable Building Material (Eberhard, Novara, & Popovec, 2018)

In addition to the cob material property tests, monolithic walls were built and tested under in-plane cyclic loading. Data was able to be recorded, and hysteresis curves were able to be developed from the loads and displacements. From these hysteresis curves, envelope curves were created which represent the stress-strain curves of the walls.
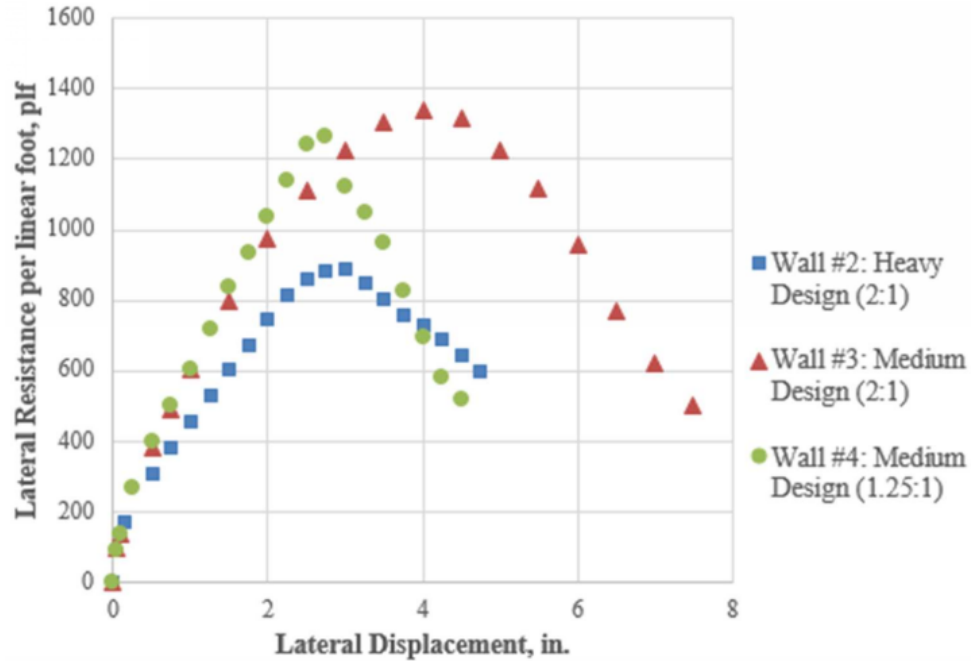
Figure 2.10: Stress-Strain Curves for Full-Scale Walls

Figure 2.10 displays the envelopes created for each wall, which can be used to solve for ductility and overall strength for each wall. This information could then be interchanged with the variables in equation (2.1), to derive an R-factor for each wall. R-values ranged from 1.5-2.5 for the three tested walls. As seen in Table 2.7, maximum applied loads and displacements at those loads were found.

$$R = R_0\sqrt{2\mu - 1} \qquad \text{(Eq. 2.1)}$$

where: $\mu = \dfrac{\Delta_u}{\Delta_y}$

$$R_0 = \dfrac{0.8V_u}{V_y}$$

15

Table 2.7: Summary of Full-Scale Wall Tests from Eberhard, Novara, & Popovec, 2018

EBERHARD, et al., 2018					
Wall	H:L Ratio	Reinforcement	Maximum Load (plf)	Displacement at Peak Loads (in)	R-factor
4	1.25:1	Medium	1267	2.75	1.5
3	2:1	Medium	1340	4	2.5
2	2:1	Heavy	887	3	2

Analyzing all the data provided, wall 2 experiences the lowest maximum load before failure. This could be a result of the large amount of reinforcement and the low bond that formed between it and the cob. Wall 3 resulted in the largest peak lateral resistance per linear force and was the most ductile of the samples. The use of additional rebar concludes a larger deflection but a decrease in maximum applied load. A common failure mechanism witnessed throughout these tests was along a lift. This could be a result of inproper interlocking of the two lifts. Lifts are necessary to increase strength of cob to prevent buldging, however, dry and wet cob do not mix well.

2.7.   Prior Research Conclusion

Compiling all the data from this chapter into one table can be seen below in Table 2.8. The data from Miccoli, Fontana, and Muller were converted to US Customary units to be compared to other results in this chapter. Table 2.8 provides a set of values that can be compared to those found in this thesis.

Table 2.8: Summary of all Prior Research

SUMMARY OF PRIOR RESEARCH*					
Resource	Density (lb/ft^3)	Compressive Strengths (psi)	Flexural Strengths (psi)	Tensile Strengths (psi)	Modulus of Elasticity (psi)
RIZZA AND BÖTTGER, 2013	92.5	96	74	26	10,371
PULLEN AND SCHOLZ, 2011	96	102	25	-	11,000
MICCOLI, et al., 2014	92	231	-	73	94,420
BRUNELLO, et al., 2018	-	126	54	-	-

3. WALL MATERIALS

This chapter reviews each material used in the wall construction. Materials used for the portable frame construction will be discussed in Chapter 5. The materials here are discussed as constituent materials (e.g. clay, sand, etc.) and then again as composite materials (e.g. cob, concrete, etc.). Included are source, summary of use, material properties, testing methods used to determine the properties, and means of production where necessary.

3.1. Constituent Materials

This section evaluates the raw materials used to create the composite materials of the pipe stem wall.

3.1.1. Clay Subsoil

The clay subsoil used in the cob mixture was obtained on the Quail Springs Permaculture property near Ventucopa, California. Figure 3.1 depicts the location of excavation. Excavation of the soil occurred around July 20, 2018 and was kept in a pile near the construction site for a week while being frequently used.

Figure 3.1: Quail Spring Soil Excavation Site (adapted from Google, 2019)

3.1.1.1. Material Properties

Grace Paananen and Lauren Becker, Cal Poly students in the geotechnical program, performed the following laboratory tests on the clay subsoil:

- ASTM D422 – Standard Test Method for Particle-Size Analysis of Soils

- ASTM D2487- Standard Practice for Classification of Soils for Engineering Purposes

- ASTM D854- Standard Test Methods for Specific Gravity of Soil Solids by Water Pycnometer

- ASTM D4318- Standard Test Methods for Liquid Limit, Plastic Limit, and Plasticity Index of Soils

The results from these tests are summarized in Table 3.1, Table 3.2 and Figure 3.2. These values resulted in a classification of the soil as a Moist Tan Lean Clay with Gravel and a specific gravity of 2.75. Detailed data from these tests and the graphs necessary for the analysis are shown in Appendix A.

Holtz' equation (4.1) classifies the clay as "inactive" from an activity, A, value of 0.7173 (133). A liquidity index, LI, is found to be less than zero, resulting in a brittle material when exposed to shear forces (Holtz et al. 46). From Figure (6.18), the soil was concluded to have a medium expansion potential (Holtz et al. 239).

Table 3.1: Quail Spring Soil Properties

SUMMARY	
Liquid Limt	35
Plastic Limit	18
Plasticity Ind.	17

Table 3.2: Quail Spring Soil Grain Size

Clay (%)	Silt (%)	Sand (%)	Gravel (%)
14.8	39.4	8.2	37.6
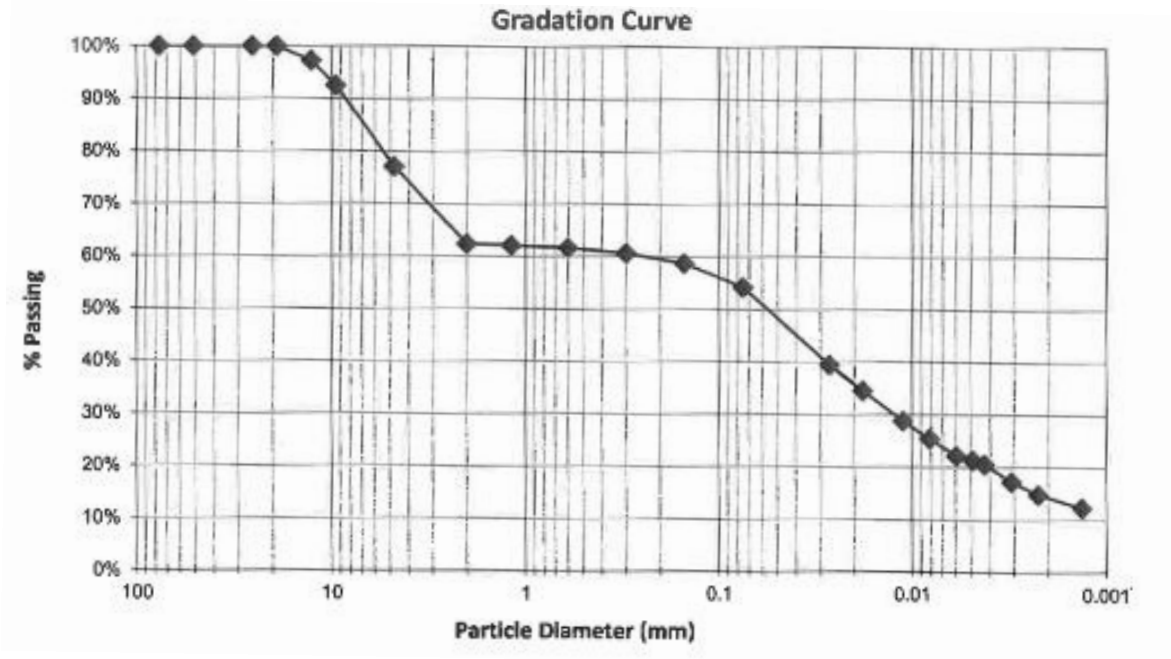
Figure 3.2: Quail Spring Soil Gradation

3.1.2. Sand

The sand used in the cob mixture came from GPS Ventucopa Rock Plant located near the

Quail Spring Permaculture property where the walls were constructed. The sand was mined

from the Cuyama River.

Figure 3.3: GPS Sand Site Map (adapted from Google, 2019)

3.1.2.1. Material Properties

The following laboratory tests were performed on the sand:

- ASTM D2487 – Standard Practice for Classification of Soils for Engineering

Table 3.3 and Figure 3.3 summarize the average results from ASTM D2487. Appendix A has multiple detailed tests and the flow chart used to classify the sand. The results classified the sand as a poorly-graded sand (SP).

Table 3.3: Cuyama River Sand Grain Size

Clay (%)	Silt (%)	Sand (%)	Gravel (%)
0	1	95	4
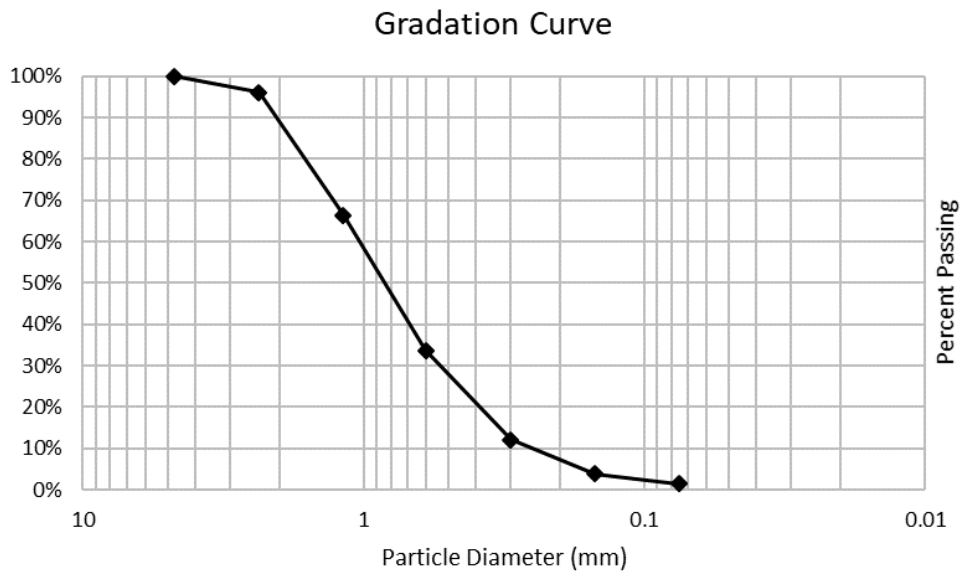
Figure 3.4: Cuyama River Sand Gradation

3.1.3. Oat Straw

The oat straw used in the cob mixture was ordered from Wachter Hay & Grain, located in downtown Ojai, Ca. It was requested to be as long as possible, around 12" to 14" in length. The straw was used as a reinforcing fiber in the cob mixture. During cob mixture, the straw was kept covered to remain dry and maintain its strength.

3.1.4. Water

All water was drawn from the Quail Spring Permaculture plumbing system. Water was used in the cob mixture, concrete, and hydrostone to achieve the correct consistency.

3.1.5. Portland Cement

All Portland cement was type II manufactured by Portland Cement Association. Cement was kept in a shed in its original sealed bag prior to use. Cement was used in the concrete for the foundation and wall topper.

3.1.6. Gravel

Gravel was acquired from GPS Ventucopa Rock Plant, like the sand. The gravel was used as large aggregate in the small batches of concrete, with the largest size being ¾".

3.1.7. Hydrostone

All hydrostone gypsum cement was manufactured by United States Gypsum Corporation (USG). After the hydrostone is given enough time to dry, a compressive strength of 10,000 psi can be reached, as seen in Table 3.4. Hydrostone was used to assist in connecting the steel channels to the concrete topper.

Table 3.4: USG Hydrostone Gypsum Specs

HYDROSTONE SPECS		
Properties	Values	Unit
1 HR. Compressive Strength	4000	psi
Dry Compressive Strength	10000	psi
Maximum Setting Expansion	0.24%	
Density Wet	108	lb/ft^3
Set Time	17-20	min

3.2. Cob

Cob consists of clay subsoil, sand, straw, and water. As discussed in Section 1.1, there are two different methods when mixing cob: British cob and Oregon cob. Oregon cob utilizes more precise measurements of the materials to create more consistent batches.

3.2.1. Oregon Cob Mixing Procedure

This section will discuss, in detail, the steps taken to create a batch of Oregon cob.

3.2.1.1. Ingredients Purposes

Clay is used to bind the materials of cob together. Enough water is needed so the clay can coat the sand and straw, and as it dries, the clay can hold the aggregates through suction. As discussed in section 1.1, clay is an unstable material due to its constant expansion and compression. To offset these rapid changes, the straw and sand are added as reinforcement to stabilize the clay and reduce cracking.

With the introduction of aggregates for stability, the more angular the sand, the better the bond with the clay due to the friction created. As for the straw, the best fibers are fresh, long, and strong. The straw should not be brittle where it will break easily or wet where it loses its integrity. The straw itself acts as a natural reinforcement, providing the cob tensile and shear strength, ductility, and insulation.

3.2.1.2. Tractor Mixing Procedure

Due to the larger scale of these tests and a need to reduce the construction time, the mixing of the cob was done via the tractor method. Since the scooping and mixing were done with the tractor, the mixture could only be as accurate and consistent as the tractor allowed.

The tractor did the initial scooping of each substance, and the crew added/removed material in the bucket, as necessary, to maintain consistent portions. The tractor was used in several different ways to mix the materials together: the bucket was used to turn the material over itself, the tires were used to drive over the mixture, and the bucket was again used to smack the cob.

Initially, a dry mixture of the sand and clay was prepared. Quail Spring Permaculture used a ratio of two sands per one clay. Where an ideal ratio is typically 20% clay to 80% sand

(Weismann & Bryce, 53), the clay subsoil used in this test already contained sand particles, and therefore, not as much additional sand was needed to offset the clay. After the dry mixture was thoroughly blended, water was added to the mixture. The tractor was used to modestly blend the materials, and then the damp mixture was left for several hours, or overnight, to allow the water to be soaked into the dry materials. When mixing continued, water and straw were continuously added to the mix in small increments until a proper consistency was met through touch. This occurred when the cob was wet enough to stick to itself and not crumble, but dry enough not to slump under its own self-weight.

The cob mixtures were made whenever a previous mixture was used. These mixtures lasted about a day, sometimes longer. When the cob needed to be used the next day, it was covered by a tarp to prevent from drying out. However, if the cob was still able to dry out, water was added to the mixture and blended into the appropriate consistency again.

From each batch, three 8"x8"x24" blocks and four 3.5" cubes were made to perform modulus of rupture tests. Blocks from each batch were made to check consistency between batches, and multiple blocks/cubes per batch were made to find an average of each batch and again check consistency.

3.2.2. Modulus of Rupture

Due to the minimal research on cob, there are no proper tests that are used to determine Modulus of Rupture of cob. Like research discussed in section 2.6., the modulus of rupture calculated in this report follow the methods set up for concrete in ASTM C293 – Standard Test Method for Flexural Strength of Concrete (Using Simple Beam with Center-Point Loading). The set up for the flexural test can be seen in Figure 3.5:
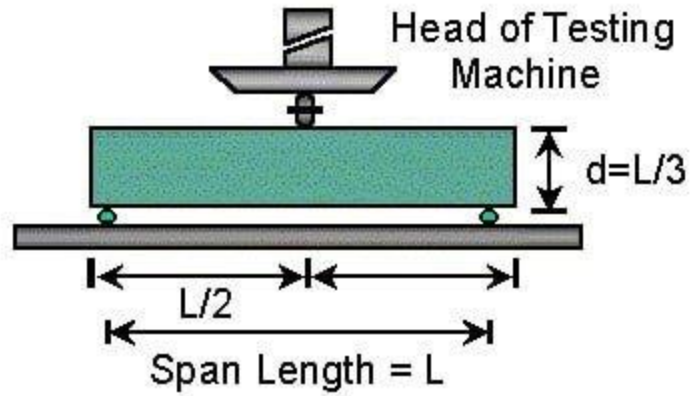
Figure 3.5: ASTM C293 Test Setup

The modulus of rupture tests were performed in two different styles. The standard setup for these tests requires a pin and roller pairing for the reaction points. However, fearful that the cob would not overcome the friction created between it and the reactions, tests were also performed with a roller and roller pairing for the reactions. These two different setups are pictured in Figure 3.6 and Figure 3.7.

Figure 3.6: Pin and Roller Reactions, before (left) and after (right)

Figure 3.7: Roller and Roller Reactions, before (left) and after (right)
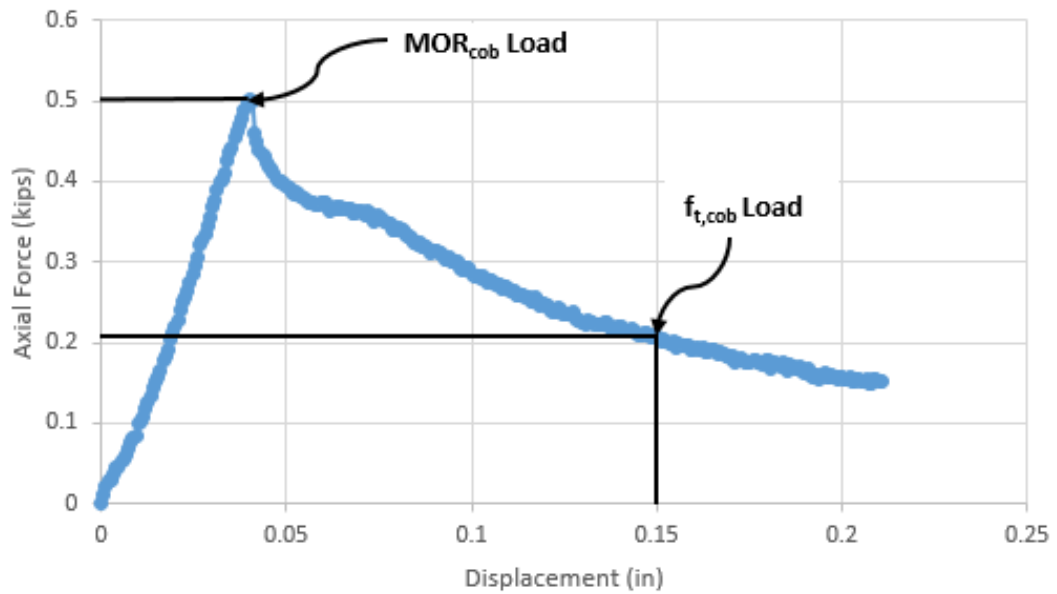
Figure 3.8: Sample 3B MOR Force vs Displacement

The compressive load was applied at a rate of 0.04 in/min. Detailed data collected can be found in appendix B, but an example of a Force versus Displacement graph can be seen in Figure 3.8. When calculating the modulus of rupture, the important details to note were the peak loads and the distance from the center in which the cracks were formed. Using this information, a maximum moment at the location of the crack can be determined. Using Equation 3.1 the modulus of rupture for each block was found and is summarized in Table 3.5.

$$MOR_{cob} = \frac{Mc}{I}$$ (Eq. 3.1)

where: M is the moment at the crack location

c is the distance from the neutral axis to furthest point

and I is the moment of inertia $\frac{1}{12}bh^3$

From the data collected, a tensile strength of the cob could also be estimated. These values were found utilizing each sample's load at 0.15 inches of displacement, shown in Figure 3.8. A displacement of 0.15 inches was chosen because it occurred far enough after the load drop where the cob strength would be dependent on the straw. The load found from the graph was then used to analyze static equilibrium and determine the internal force of the cob. These forces were then used in Equation 3.2 to determine the cob tensile strength. A ratio of the tensile strength to modulus of rupture was then found using Equation 3.3.

$$f_{t,cob} = \frac{P}{A}$$ (Eq. 3.2)

$$\frac{f_{t,cob}}{MOR_{cob}}$$ (Eq. 3.3)

The following data in Table 3.5 is missing information for block 2-C because it was lost in transit and information from block 6-A because it was considered an outlier. Average modulus of rupture and tensile strength values for these cob mixtures were found to be 33 psi and 23 psi, respectively. Compared to those values displayed in Table 2.8, the modulus of rupture calculated in this research is within range and the tensile strength appears reasonable. Table 3.6 compares those values and presents the percent differences.

Table 3.5: Average Fracture Strength from Modulus of Rupture Tests

SUMMARY OF MOR TESTS			
Name	MOR_{cob} (psi)	$f_{t,cob}$ (psi)	$f_{t,cob}/MOR_{cob}$
1-A	40.32	24.31	60%
1-B	30.58	25.22	82%
1-C	25.00	23.41	94%
2-A	22.74	13.28	58%
2-B	28.75	14.99	52%
2-C	-	-	-
3-A	29.95	34.04	114%
3-B	32.54	18.61	57%
3-C	41.31	38.29	93%
4-A	34.90	-	-
4-B	41.90	34.05	81%
4-C	39.47	30.84	78%
5-A	34.14	24.1	71%
5-B	21.62	17.56	81%
5-C	34.87	29.44	84%
6-A	10.88	11.07	102%
6-B	38.24	18.05	47%
6-C	32.52	14.7	45%
Max	41.90	38.29	114%
Min	21.62	11.07	45%
Average	33.05	23.25	73%
St. Dev	6.39	8.29	20%
95% Confidence	3.13	4.20	-

Table 3.6: MOR Test Comparison to Prior Research

MOR TEST COMPARISON				
Resource	Flexural Strengths (psi)	% Difference Flexural Strength Compared to this Report	Tensile Strengths (psi)	% Difference Tensile Strength Compared to this Report
THIS REPORT	33	0%	23	0%
RIZZA AND BÖTTGER, 2013	74	123%	26	12%
PULLEN AND SCHOLZ, 2011	25	24%	-	-
MICCOLI, et al., 2014	-	-	73	212%
BRUNELLO, et al., 2018	54	65%	-	-

From Table 3.5, its apparent that cob has inconsistent performances due to the variability in mixtures. Table 3.7 calculates the average modulus of rupture and tensile strengths for each batch, as well as their standard deviations. These values show that even within each batch, these cob properties can fluctuate due to aspects as simple as uneven distribution of straw. This is the nature of cob. However, comparing the values between batches, the modulus of rupture and tensile strengths are consistent enough that the mixing procedure is efficient.

Table 3.7: MOR Test Batch Comparisons

Average Name	Average MOR_{cob} (psi)	St. Dev	Average $f_{t,cob}$ (psi)	St. Dev	Average $f_{t,cob}/MOR_{cob}$
Batch 1	31.96	7.75	24.31	0.91	76%
Batch 2	25.75	4.25	14.14	1.21	55%
Batch 3	34.60	5.96	30.31	10.36	88%
Batch 4	38.76	3.55	32.45	2.27	84%
Batch 5	30.21	7.45	23.70	5.95	78%
Batch 6	35.38	4.04	16.38	2.37	46%

3.2.3. Density, Compressive Strength, and Moisture Content

Compression tests were performed following a modified procedure of ASTM C39. Further details of how the test was conducted and the data collected can be found in Julia Sargent's thesis (2019). Figure 3.9 displays the setups for the compressive strength tests. A summary of the results can be found in Table 3.7. From this table, an average compressive strength and Modulus of Elasticity were found to be 174 psi and 31,316 psi, respectively. These values were compared to those from Table 2.8, and their percent differences can be seen in Table 3.8. These values are graphed in Figure 3.10 to demonstrate that the modulus of elasticity increases linearly to the compressive strength. The unit weight, moisture content, and Poisson's ratio values were found to be 107.3 pcf, 1.6%, and 0.172 respectively.
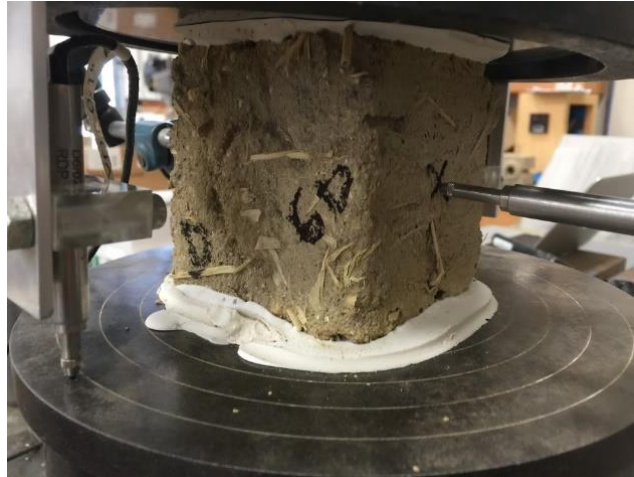
Figure 3.9: Vertical and Horizontal Displacement

Table 3.8: Average Compressive Strengths

SUMMARY OF COMPRESSIVE STRENGTH TESTS					
Sample	Unit Weight (lbs/ft^3)	Compressive Strength (psi)	LVDT M.o.E. (psi)	Moisture Content (%)	Poisson's Ratio
Average	107.3	174	39,369	1.6%	0.172
St. Dev.	7.0	25	7,204	0.5%	0.042
Min	84.7	113	8,270	0.6%	0.113
Max	116.7	227	49,252	2.2%	0.220

Table 3.9: Compressive Strength Test Comparison

COMPRESSIVE STRENGTH TEST COMPARISON				
Resource	Compressive Strengths (psi)	% Difference Compressive Strengths Compared to this Report	Modulus of Elasticity (psi)	% Difference MOE Compared to this Report
THIS REPORT	174	0%	39,369	0%
RIZZA AND BÖTTGER, 2013	96	45%	10,371	74%
PULLEN AND SCHOLZ, 2011	102	41%	11,000	72%
MICCOLI, et al., 2014	231	33%	94,420	140%
BRUNELLO, et al., 2018	126	28%	-	-

$$y = 598.05x - 51249$$
$$R^2 = 0.9439$$
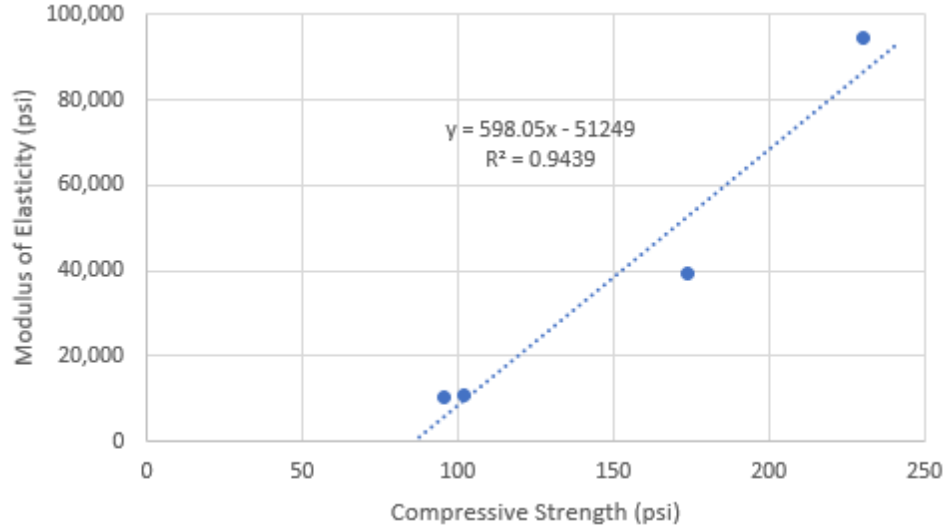
Figure 3.10: Modulus of Elasticity and Compressive Strength Relationship

3.3. Reinforcing Steel Pipes

The steel pipes used as the main reinforcing component of the pipe stem wall were purchased from Ventura Steel. A mill certificate was provided for the 2-1/2" pipes from the Far East Machinery Co, Ltd, in Taiwan.

Figure 3.11: Material Properties of 2-1/2" Recycled Pipes

3.4. Welded Wire Steel Reinforcement

The welded wire steel reinforcement, or steel mesh, used as another reinforcing component for the cob wall was purchased from Davis Wire Corporation. A Certificate of Compliance was provided for the 6x6 W2.9/W2.9 steel mesh which can be seen in Figure 3.11. Per ASTM A1064, a minimum (ultimate) tensile strength of 80,000 psi is satisfied and therefore it is supported that the yield strength of the welded wire steel will be greater than 70,000 psi.

DAVIS WIRE CORPORATION
A HEICO WIRE GROUP COMPANY
P.O. Box 2145 Irwindale, California 91706-1097
PHONE (626) 969-7651 • FAX (626)334-4780

CERTIFICATE OF COMPLIANCE

DATE: 6/12/2018

CUSTOMER: HD SUPPLY WHITE CAP - S. CAL
MATERIALS DESCRIPTION: CF 6X6 W2.9/W2.9 7FX20F PNL

CUSTOMER ORDER NO. 2809892
DAVIS WIRE ORDER NO. S054187
PROJECT:

SPECIFICATION: A-1064

	HEAT#	C	Mn	P	S	Si
LINE WIRE	8A16313	0.140	0.450	0.019	0.021	0.130
CROSS WIRE	8A16313	0.140	0.450	0.019	0.021	0.130

	DIAMETER (in.)	R.A (%)	BREAK (LBf)	TENSILE (ksi)	BEND (WRAPS) 5X MANDREL	WELD SHEAR average (lbf)	WELD SHEAR average (lbf)
LINE WIRE	0.192	56.3	2737	94.4	PASS	2288	2629
CROSS WIRE	0.192	56	2710	93.4	PASS	2656	2770
						2979	2536
						2655	----
						2596	----
						2576	----
						2551	----
						AVERAGE:	2624

REMARK:
150 PANELS

Materials attested to above have been produced to the best industry practices and in all respects comply with the above stated specification. We hereby certify that the above test results are representative of those contained in the records of the company and were obtained using methods consistent with the requirements of applicable specification listed above.
Above products were manufactured in the U.S.A

X _____ Matthew Allen Quality Assurance Supervisor

6/12/2018 Date

The emplyee signing above has the legal authority to certify this material on behalf of Davis Wire Corporation.

Figure 3.12: Material Properties of 6x6 Steel Mesh

3.5. Foundation and Top Beam Concrete

The concrete for the foundation had the mixture ratio of 3-parts sands, 2-parts gravels, and 1-part cement. The concrete foundations and top beams were reinforced to ensure that the failure of the test would not occur in the concrete additions. The foundation contained some of the reinforcing steel pipes from section 3.3, and the top beam was reinforced with #4 rebars. These are further discussed with respective images to illustrate the reinforcement in chapter 4.

4.   WALL CONSTRUCTION

This section describes the steps taken to construct the pipe stem wall. The construction occurred during the summer of 2018 at Quail Springs Permaculture near Ventucopa, California.

4.1.   Recycled Steel Pipe Reinforcement

Preceding cob mixture and wall construction, the recycled steel pipe reinforcement size and layout needed to be selected. Art Ludwig of Oasis Design chose the mockup displayed in Figure 4.1. Complete architectural drawings for this wall can be found in appendix C. Table 4.1 also provides typical dimensions for the reinforcement.
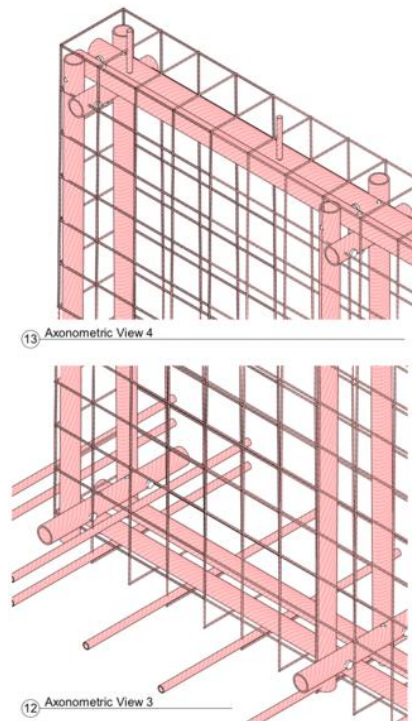
Figure 4.1: Architectural Drawings of Reinforcement

Table 4.1: Dimensions of Reinforcement

WALL REINFORCEMENT	
Properties	**Values**
Mesh Long Spacing	6"x6"
Mesh Short Spacing	1'-1/16"
Pipe Long Spacing	3'-4"
Pipe Short Spacing	9-1/8"

The 2-1/2" steel pipe reinforcement experienced modifications to allow the orientation in Figure 4.1. The fabrication of the reinforcement, such as drilling and slotting holes, was executed by Art Ludwig and can be seen in Figure 4.2. Once the pipe reinforcing was assembled, the wire mesh could be arranged around it. The result of the reinforcement placed in the foundation form can be observed in Figure 4.3.

Figure 4.2: Fabrication of the Recycled Steel Reinforcement

Figure 4.3: Complete Reinforcement in Foundation Form

4.2.   Construction Procedure

Once the reinforcement was placed, the foundation was mixed and poured, following the portions described in section 3.5. The form was constructed to create a concrete base that was 22 inches thick, 8 inches deep, and 110 inches long. The concrete was left to cure for one day before the cob wall was built on top of it. The cob being constructed on the concrete applies a small load to the concrete, which was assumed not to affect the strength of the concrete. Before any testing occurred, the concrete was able to reach its full potential strength with a curing period greater than the 28-day minimum.

The cob used for the wall followed the same mixing procedure discussed in section 3.2.1.2. Once the cob was fully mixed, the wall could be constructed around the reinforcement in lifts of roughly one foot. As discussed in section 1.1., British cob allows their lifts to dry for 2 weeks before the addition of a new lift. For this test, each lift was left to dry for a maximum of 1 day. Since the wall was constructed during the hot days of July, the surrounding environment was so dry that sometimes a lift could be formed in the morning and another one could be completed before the end of the day. To ensure a strong bond between lifts, the top of each lift was covered to keep that layer moist during the drying period. After an allotted time, the previous layer was punctured with thumb sized holes and the next layer was thumbed into it to interlock the straw. Figure 4.4 demonstrates the technique used to manage a moist top layer, and Table 4.2 describes the construction timeline.

Figure 4.4: Cob Lifts

Table 4.2: Lift Information

CONSTRUCTION TIMELINE	
Date	**Event**
Prior to 7/23/2018	Fabricate Reinforcement Frame
7/23/2018 2:46 PM	Erect Frame in Foundation Form
7/23/2018 3:36 PM	Begin Pouring Foundation
7/23/2018 5:30 PM	Complete Foundation Pour
7/25/2018 EOD	Complete 19 inches
7/26/2018 EOD	Complete 31 inches
7/27/2018 EOD	Complete 52 inches
7/28/2018 EOD	Complete71 inches
7/29/2018 EOD	Complete Wall
*EOD = End of Day	

4.3.   Reinforced Concrete Top Beam

Since this research paper was only a portion of the overall project performed, the

overall project was taken into consideration when building this wall. The portable loading frame,

that will be further discussed in Chapter 5, was designed to be put together the same way every

time. In order to achieve this, all the walls needed to be the same height. Since the walls were

formed by hand, there was ample room for human error. To counteract the error, a reinforced

concrete top beam was added to all the walls to bring their heights to 7'-9". The beams were

reinforced with #4 bars to ensure they will not be the failing factor. Figure 4.5 spotlights this

through the multiple bars shown. After pouring the concrete, the bristles from a broom were

used to roughen the top layer of the concrete, shown in Figure 4.6.

Figure 4.5: Concrete Reinforcement

Figure 4.6: Roughed-Up Concrete Beam

4.4. Steel Loading Channels

With the wall construction thus far, there is no actual point established to apply the force from the loading frame. To connect the two components, two C4X5.4 channels were attached to the top beam with 5/8" welded plates acting as a clevis. The pin from the loading frame was then able to connect to the channels and transfer the loads. The connection of these two components will be further discussed in Chapter 5 accompanied by a picture of the connection.

To secure the channels with the top beam, there were multiple forms of connection points. Figure 4.7 is a CAD replica of the plan view of the channels. The first form of connection to note are the seven holes drilled into the channels that were replicated onto the top beams. These holes were drilled onto the concrete top beams in the same pattern as shown below with a minimum spacing between the plates of three inches. The holes were then filled with epoxy and a thread rod was inserted. Once dried, the channels were placed on the top beam with the thread rods going through the holes on the channels. The channels were then fixed in place with washers and nuts to accompany the thread rods.
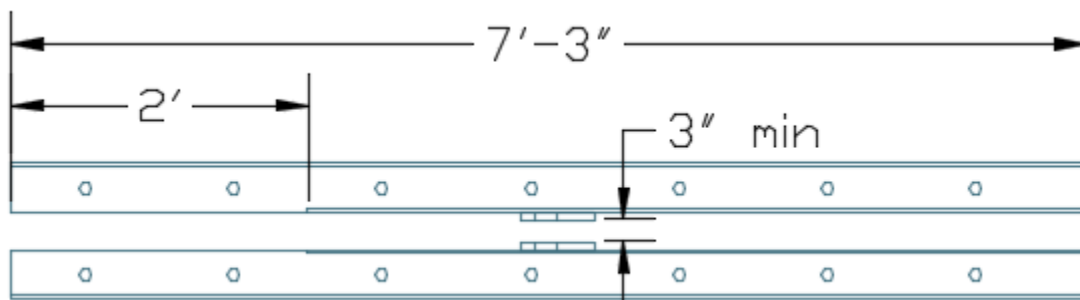
Figure 4.7: CAD of Channels, Plan View

The second form of connection was hydrostone. Hydrostone was mixed to a thin, pancake-like consistency. It was then poured onto the top beam and spread to fill all the gaps between the channels and the concrete top beam. This method eliminated the potential for

settlement from the channels and any sliding between the two members. Figure 4.8 shows the

channels after they had been anchored down with the thread rods and the hydrostone.

Figure 4.8: Anchored Channels

5. FRAME CONSTRUCTION

5.1. Predicted Load Calculations

To design the loading frame, a maximum applied load needed to be predicted. This was achieved by analyzing the global equilibrium of the wall, assuming a location of the applied load at the top of the wall and material properties of the cob wall. Accepting data from section 2.8, a conservative tensile strength of 100 psi was used, and incorporating the density from section 3.2.3, a weight of 8,000 lbs was presumed. Figure 5.1 illustrates the different loads used to analyze global equilibrium.
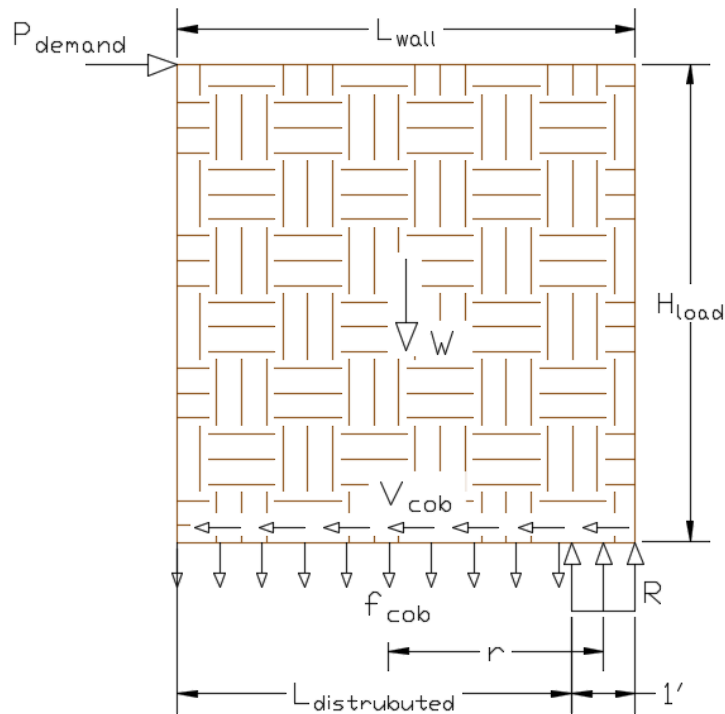
Figure 5.1: Global Equilibrium of the Cob Wall

Regarding Figure 5.1, utilize the sum of the forces in the vertical direction:

$$\sum F_y = 0 = R(1\ ft) - W - f_{cob}(t)(L_{distributed}) \quad \text{(Eq. 5.1)}$$

where   R is the foundation reaction distributed load

W is the weight of the cob wall

f_{cob} is the cob tensile strength

t is the wall thickness

$L_{distributed}$ is the length the tensile distributed load was applied

Rearrange equation 5.1 to solve for the foundation reaction forces:

$$R = \frac{W + f_{cob}(t)(L_{distributed})}{1\,ft} \tag{Eq. 5.2}$$

The foundation reaction force was found to be **108.8 kips**.

Evaluate a moment about the location of the reaction force:

$$\sum M_R = 0 = W\left(\tfrac{1}{2}L_{wall} - \tfrac{1}{2}"\right) + f_{cob}(t)(L_{distributed})(r) - P_{demand}(H_{Load}) \tag{Eq. 5.3}$$

Rearrange equation 5.3 to solve for the predicted maximum applied load:

$$P_{predicted} = \frac{W\left(\tfrac{1}{2}L_{wall} - \tfrac{1}{2}"\right) + f_{cob}(t)(L_{distributed})(r)}{(H_{Load})} \tag{Eq. 5.4}$$

where $P_{predicted}$ is the predicted maximum applied load of the wall

W is the weight of the cob wall

L_{wall} is the length of the wall

f_{cob} is the tensile strength of the cob

$L_{distributed}$ is the length of the distributed tensile strength

r is the moment arm of the distributed load

H_{Load} is the height to the applied load

The predicted maximum load the wall could withstand was found to be 47.1 kips. To be conservative, the maximum load used to design the loading frame was **60 kips**.

The last equation to analyze from the global equilibrium was the sum of the forces in the horizontal direction:

$$\sum F_x = 0 = P_{predicted} - V_{cob}(L_{wall}) \tag{Eq. 5.5}$$

where $P_{predicted}$ is the predicted maximum applied load of the wall

V_{cob} is the predicted shear capacity of the cob

L_{wall} is the length of the wall

Rearrange equation 5.5 so the shear capacity of the cob could be predicted:

$$V_{cob} = \frac{P}{L_{wall}}$$ (Eq. 5.6)

A shear capacity of 6.73 k/ft was found.

Table 5.1: Predicted Load Capacities

ESTIMATE LOAD CAPACITY			
Item	Variable	Value	Unit
Foundation Reaction	R	108.8	k
Predicted Maximum Hydraulic Jack Force	P_{demand}	47100	lbs
		47.100	k
Force used in Calcs	P_{design}	60	k
Force in Each Column		30	k

5.2.   Frame Design Calculations

Regarding the design of the loading frame, key concepts needed to be achieved. The loading frame had to apply a load of up to 60 kips, in order to reach the predicted load and cause failure of the wall. The cob walls were built hundreds of miles from campus and each weighed approximately 8,000 lbs; a vital concept of the loading frame was that it must be easily transported and put together. In a previous thesis at Cal Poly, a frame design of columns with support kickers was used. Those pieces could be recycled and reused for this report, but an analysis of their capacity needed to be performed. Figure 5.2a, Figure 5.2b, and Figure 5.3 illustrate the different sections of the loading frame and their respective loads.
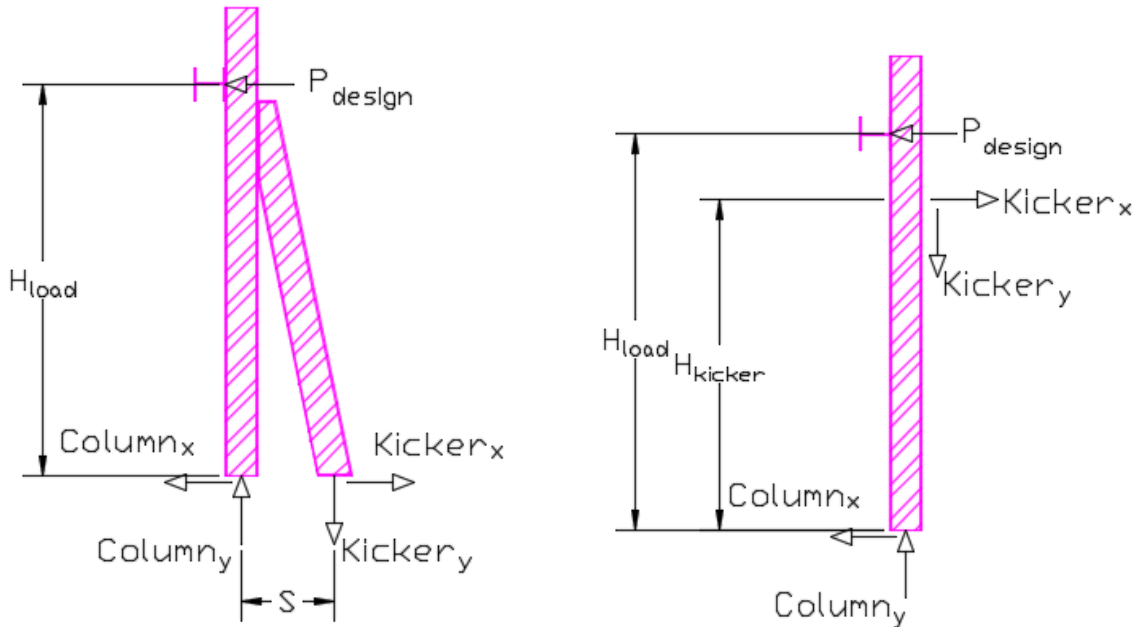
Figure 5.2: a) Column and Kicker Free Body Diagrams b) Column Free Body Diagram

Regarding Figure 5.2a, consider a moment about the bottom of the column:

$$\sum M_{bottom\ column} = 0 = P_{design}(H_{Load}) - Kicker_y(S) \qquad \text{(Eq. 5.7)}$$

where P_{design} is the design applied load on the wall

H_{Load} is the height of the location of the applied load

$Kicker_y$ is the reaction of the kicker in the vertical direction

S is the spacing between the foot of the column and the kicker

Rearrange equation 5.7 to solve for the reaction of the kicker in the vertical direction:

$$Kicker_y = \frac{P_{design}(H_{Load})}{S} \qquad \text{(Eq. 5.8)}$$

Evaluate the sum of the forces in the vertical direction:

$$\sum F_y = 0 = Column_y - Kicker_y \qquad \text{(Eq. 5.9)}$$

where $Column_y$ is the reaction of the column in the vertical direction

$Kicker_y$ is the reaction of the kicker in the vertical direction

Rearrange equation 5.9 to solve for the reaction of the column in the vertical direction:

$$Column_y = Kicker_y \qquad \text{(Eq. 5.10)}$$

Regarding Figure 5.2b, examine a moment about the bottom of the column:

$$\sum M_{bottom\ column} = 0 = P_{design}(H_{Load}) - Kicker_x(H_{Kicker}) \qquad \text{(Eq. 5.11)}$$

where P_{design} is the design applied load on the wall

H_{Load} is the height of the location of the applied load

$Kicker_x$ is the reaction of the kicker in the horizontal direction

H_{Kicker} is the height to the connection point of the kicker of the column

Rearrange equation 5.11 to solve for the force of the kicker in the horizontal direction:

$$Kicker_x = \frac{P_{design}(H_{Load})}{H_{Kicker}} \qquad \text{(Eq. 5.12)}$$

Investigate the sum of the forces in the horizontal direction:

$$\sum F_x = 0 = Kicker_x - Column_x - P_{design} \qquad \text{(Eq. 5.13)}$$

where $Kicker_x$ is the reaction of the kicker in the horizontal direction

$Column_x$ is the reaction of the column in the horizontal direction

P_{design} is the design applied load on the wall

Rearrange equation 5.13 to solve for the force of the column in the horizontal direction:

$$Column_x = Kicker_x - P \qquad \text{(Eq. 5.14)}$$

Table 5.2: Horizontal and Vertical Forces in Column and Kicker

CALCULATE REACTIONS AT CONNECTIONS			
Item	Variable	Value	Unit
Y Force in Kicker	$Kicker_y$	-120	k
Y Force in Column	$Column_y$	120	k
X Force in Kicker	$Kicker_x$	40	k
X Force in Column	$Column_x$	-10	k
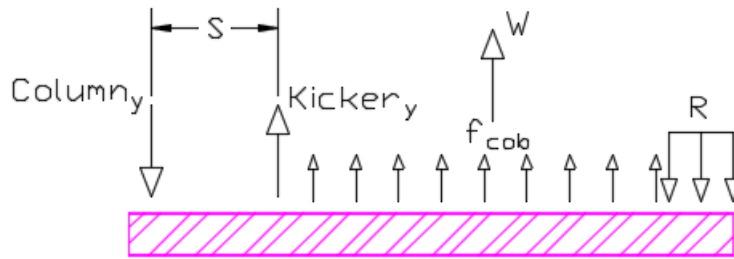
Figure 5.3: Bottom Beam Free Body Diagram

Applying the forces found in Table 5.2, a shear analysis of the column can be seen from

the diagram in Figure 5.4. Implementing Figure 5.3 and the established forces in Table 5.2, a

shear diagram of the bottom beam can be formulated in Figure 5.5. These shear forces can be

used to evaluate the stresses the W8X31 beams endure and make modifications where

necessary. The forces can also be used to decide the number and size of the bolts at each

connection point. The next sections discuss how this information was used to select each

component for the frame, as well as the material properties and the construction process

followed to ensure the frame would not fail.
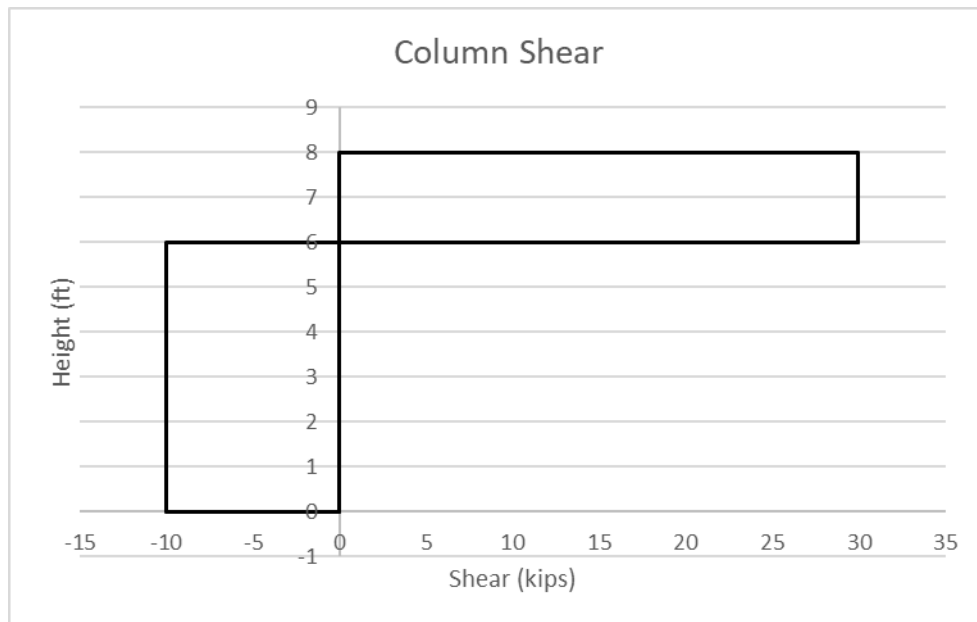
Figure 5.4: Shear Diagram of the Column

44
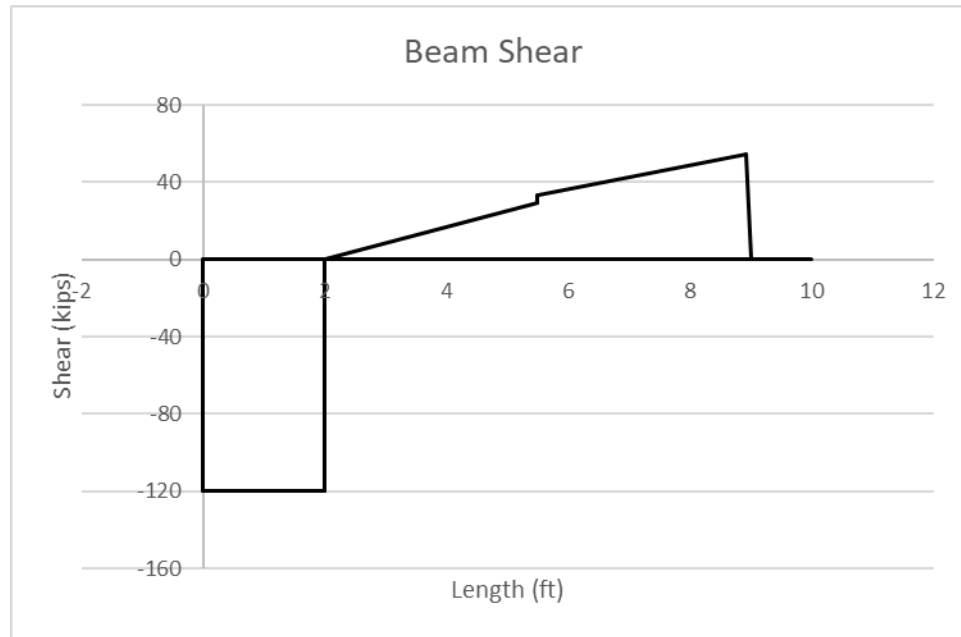
Figure 5.5: Shear Diagram of the Bottom Beam

5.3.   Frame Materials

This section discusses the materials used in the frame construction, specifically.

5.3.1. Steel

The large components of the loading frame were all steel pieces. Table 5.3 identifies the

different types of steel, with their respective material properties and descriptions of use. The

W8X31 steel pieces used for the bottom beam, column, and kickers had unknown properties, as

they were recycled pieces from a previous thesis on the Cal Poly campus. The values in the table

were chosen assuming an A36 steel type. The channels and 5/8" plates were welded together to

create the connection between the wall and the loading frame.

Table 5.3: Material Properties of Different Steel in Loading Frame

STEEL PROPERTIES					
Material	**Type**	**Yield Strength**	**Tensile Strength**	**Description of Use**	**Source**
W8x31 Steel	A36	36,000 psi	58,000 psi	Beams, columns, and kickers	Cal Poly
1/4" thick 8-1/4"x72" Steel	Hot Rolled	45,000 psi	67,000 psi	Plates welded to side of bottom beams	BB Steel
C4x5.4 Steel	Standard	36,000 psi	58,000 psi	Channels for loading frame	BB Steel
5/8" thick 5"x8-1/2" Steel	Hot Rolled	45,000 psi	67,000 psi	Plates welded to channels	BB Steel

5.3.2. Bolts and Nuts

Inspecting the information in Table 5.2 and Figure 5.4 and Figure 5.5, the pullout forces at connection points could be determined. From this, bolt sizes were chosen and their potential stresses due to the pullout forces could be calculated. Table 5.4 lists the properties for the chosen bolt sizes, including their design strengths to compare to their yielding strengths. Table 5.5 specifies the material properties of the respective nuts for each bolt size.

Table 5.4: Material Properties of Different Bolt Sizes in Loading Frame

BOLT PROPERTIES						
Size	Grade	Demand	Yield Strength	Tensile Strength	Description of Use	Source
1-1/4"-7 Steel	5	49,000 psi	92,000 psi	100,000 psi	Connection of column & kicker to bottom beams	McMaster-Carr
7/8"-9 Steel	A325	12,500 psi	92,000 psi	120,000 psi	Connection of kicker to column	Cal Poly
3/4"-10 Steel	8	23,000 psi	130,000 psi	150,000 psi	Connection of top beam to columns	McMaster-Carr
1/2"-13 Steel	5	38,500 psi	92,000 psi	120,000 psi	Connection of anchor block to top beam	Fastenal

Table 5.5: Material Properties of Different Nut Sizes in Loading Frame

NUT PROPERTIES					
Size	Grade	Yield Strength	Tensile Strength	Description of Use	Source
1-1/4"-7 Steel	5	92,000 psi	120,000 psi	Connection of column & kicker to bottom beams	Fastenal
7/8"-9 Steel		92,000 psi	120,000 psi	Connection of kicker to column	Cal Poly
3/4"-10 Steel	5	92,000 psi	120,000 psi	Connection of top beam to columns	McMaster-Carr
1/2"-13 Steel	5	92,000 psi	120,000 psi	Connection of anchor block to top beam	McMaster-Carr

5.3.3. Purchased Prefabricated Parts

Prefabricated pieces were purchased to apply the seismic load to the wall. A hydraulic jack was chosen that could generate loads up to the values found in Table 5.1. Table 5.6 displays those purchased pieces and their load capacities and Table 5.7 shows the manufacturer specs for the hydraulic jack.

Table 5.6: Material Properties of Purchased Prefabricated Parts in Loading Frame

PREFABRICATED PART PROPERTIES			
Material	Load Capacity	Description of Use	Source
1-1/2"-12 Ball Joint Rod	64,750 lb	Connection of loading frame to wall	McMaster-Carr
Hydraulic Jack	54,510 lbs	Applies loading force	Prince

Table 5.7: Specs for Hydraulic Jack

5 INCH BORE CYLINDERS							
A & B Series Royal Plate Rod	E & F Series Chrome Rod	Stroke	Wt	Column Load (lbs)	Retract	Tare Dist. (H)	Standard Dimensions of 5 Inch Bore Cylinders
B500080ACDDA07B	F500080ACDDA07B	8"	72	58900 lbs	20 ¼	4	Note: 2" rod diameter
B500120ACDDA07B	F500120ACDDA07B	12"	83	58900 lbs	24 ¼	4	Outside Sq. Dim. Butt - 5.875, Gland 5.875
B500140ACDDA07B	F500140ACDDA07B	14"	88	58900 lbs	26 ¼	4	A ¼" cylinder tube wall thickness
A500160ACDDA07B	E500160ACDDA07B	16"	96	58900 lbs	31 ½	7 ¼	B, C SAE ⅞ -14 extend & retract ports
B500180ACDDA07B	F500180ACDDA07B	18"	98	58900 lbs	30 ¼	4	D 1.265" clevis pin hole size
B500200ACDDA07B	F500200ACDDA07B	20"	103	58900 lbs	32 ¼	4	E, F 1 ¾" base clevis throat depth with 2⅝" from pin
B500240ACDDA07B	F500240ACDDA07B	24"	113	54510 lbs	36 ¼	4	center to port center
B500300ACDDA07B	F500300ACDDA07B	30"	129	37620 lbs	42 ¼	4	G 2" rod clevis throat depth
B500360ACDDA07B	F500360ACDDA07B	36"	144	27520 lbs	48 ¼	4	J 1.13" min. distance between ears at pin center line
B500480ACDDA07B	F500480ACDDA07B	48"	175	16550 lbs	60 ¼	4	K 1 ⅜" base clevis ear radius
							L 1 ¼" rod clevis ear radius
							M 1 ½" – 12 UNF-3 piston rod clevis thread size
							N 1 ⁷⁄₁₆" piston width
							O 2 ½" gland width

Seal Kits: Seal Kit for A, B, E, F & SAE-350XX Cylinder Models = PMCK-B500000
Universal Seal Kit for SAE-95XX, SAE-350XXX, A, B, E & F Cylinder Models = 240040027

5.4. Fabrication and Construction

The steel used for the beams, columns, and kickers were recycled steel used in previous theses on Cal Poly's campus. The steel needed to be adjusted to accommodate the needs in this research, and the different modifications were completed by several Cal Poly students. This section discussed the construction process of each piece for the loading frame and the modifications performed on those pieces.

5.4.1. Bottom Beam

The bottom beams were designed to hug the concrete foundation to provide a connection to the wall and take over the forces the foundation would endure. The connection occurred through (13) ¾" thread rods, which traversed the concrete foundation and latched on to the web of the W8X31 steel beams through drilled holes to match those in the foundation. In addition to the holes drilled for the thread rods, larger 1-½" holes were drilled at the locations where the columns and kickers would connect to the bottom beams.

Reviewing Figure 5.5 above, the bottom beams would experience shear forces as high as 120 kips causing a shear of about 60 ksi. To reduce the stress on the beams, a ¼" steel plate was welded to the inside of the bottom beam, which brought the stress down to about 30 ksi. Allen Lactaoen and Michael Clark, two Cal Poly students certified as campus shop technicians,

executed the welding. Holes were then drilled on the ¼" plates to align with the holes for the

traverse thread rods discussed above.

Lastly, the length of the beams extended beyond 13 feet, while the foundation was only

9 feet in length. The excess length of the beam was causing an unnecessary increase of about

100 lbs and was therefore opposing one of the key concepts for this loading frame. Cody Parker,

another shop technician at Cal Poly, assisted in the reduction of the beams to 10 feet.

Figure 5.6: Bottom Beam Side View

5.4.2. Column and Kicker

The columns and kickers were from a previous Cal Poly thesis design and were deemed

adequate for this research. The foot of the kicker was located two feet from the foot of the

column and the top of the kicker connected about six feet high on the column. (4) 7/8" bolts

were used to connect each kicker to their respective column. No modifications were made to

these parts. The columns and kickers connected to the bottom beams via (8) 1-¼" bolts. The

column and kicker combos were lifted onto the beams either by multiple people or with the

assistance of a tractor, and the bolts were screwed into place.

Figure 5.7: Column and Kicker

5.4.3. Top Beam

The top beam came from a shorter W8X31 beam that was approximately 5'-1" long. The top beam would span the two columns, on the side opposite the wall, at the height of the applied load. Since each wall is slightly different with different widths or slants, the top beam contained slotted holes drilled by Michael Clark utilizing a CNC machine. The slotted holes would allow the beam to shift horizontally to maintain an applied load in the center of the wall to eliminate any torsion. In addition, (6) ¾" holes were drilled to allow the hydraulic jack to connect to the loading frame via the anchor block.

Figure 5.8: Top Beam Side View

5.4.4. *Hydraulic Jack, Load Cell, Pin*

After the installation of the top beam, the loading application could be added. The loading application consisted of the hydraulic jack which would provide the load, the load cell which would record the applied load to the data acquisition system, and the ball joint rod which would act as a connection point to the top of the loading channels on the wall discussed in section 4.4. The hydraulic jack was connected to the top beam utilizing an anchor block and (6) ½" bolts
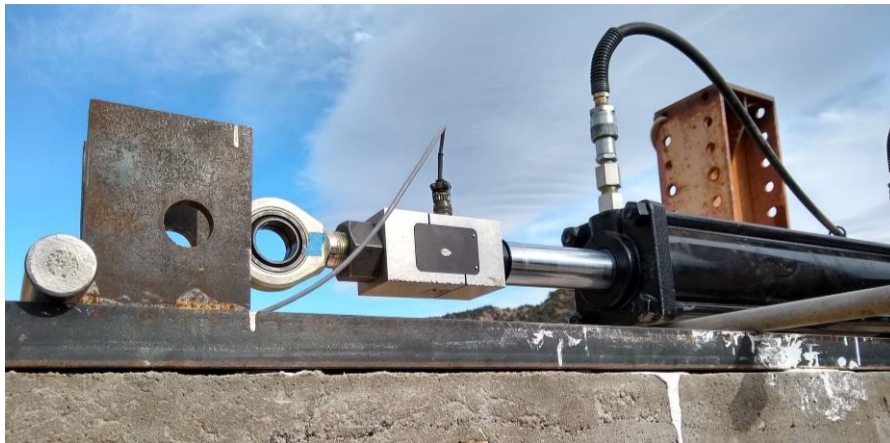
Figure 5.9: Pin (Left) Load Cell (Middle) Hydraulic Jack (Right)

6.   WALL TESTING

This chapter displays the complete setup of the test, including the instrumentation

setup and parameters being recorded. Direct data from the test are reviewed, prior to analysis

and distinct developments are inspected.

6.1.   Testing Layout

Following the frame construction process discussed in chapter 5, the final layout of the

loading frame in place around the cob wall can be viewed in Figure 6.1 as a CAD representation

and again in Figure 6.2 in real view.
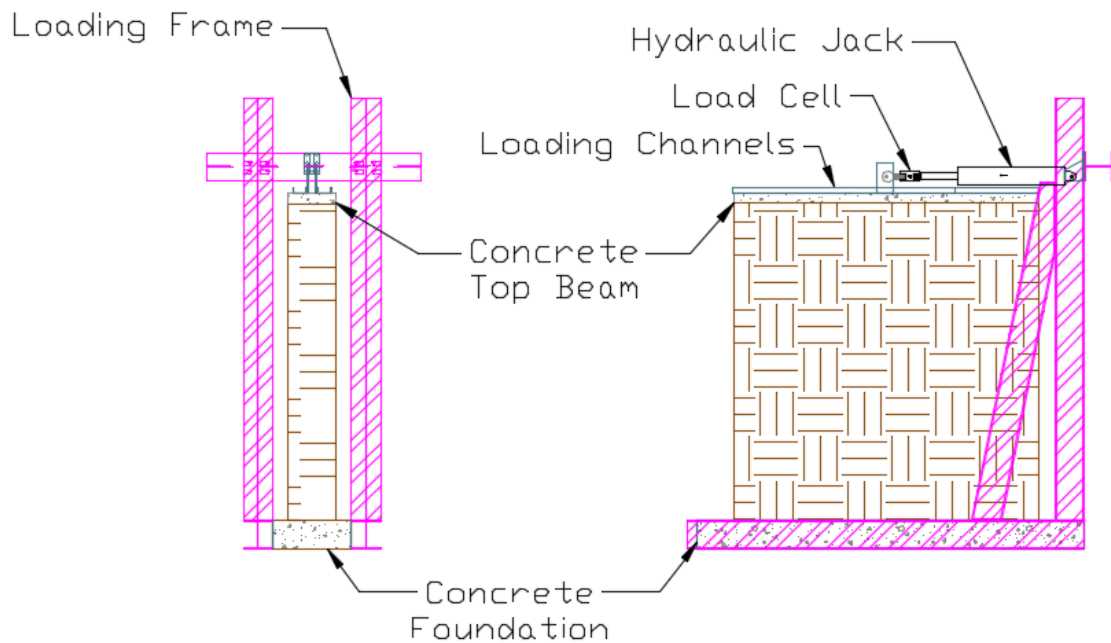
Figure 6.1: CAD of Entire Layout

Figure 6.2: Real View of Entire Layout

6.1.1. Loading Actuator

The hydraulic jack first mentioned in section 5.3.3 can provide a maximum column load of 54,510 lbs. The connection to the wall occurs while the hydraulic jack is extended around 10 inches. The hydraulic jack is capable of a 24-inch stroke, which allows the wall to be pushed up to 14 inches and pulled up to 10 inches. This provides considerable room to perform the cyclic loading. The hydraulic jack was controlled by a hand pump. With a hand pump and pressure release valves between the pump and hoses, unloading the loads could be controlled to attempt to prevent the cob from springing back to its position prior to that cycle.
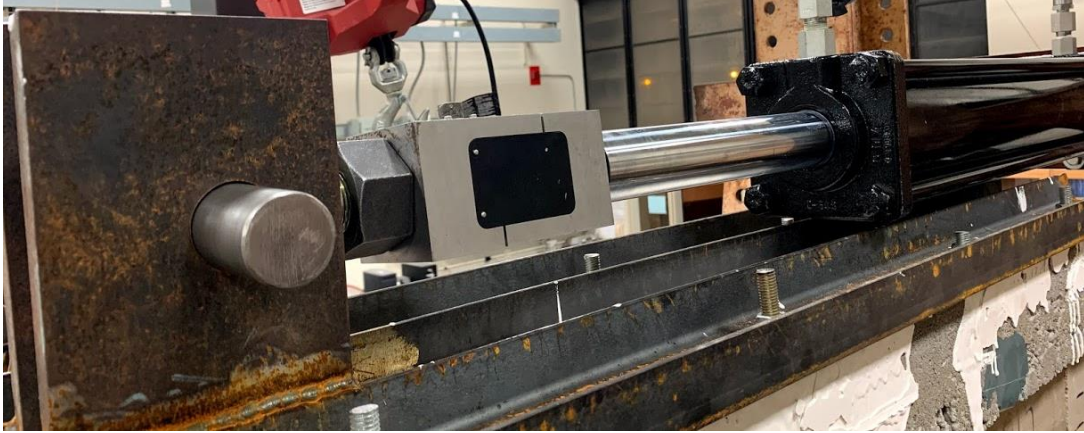
Figure 6.3: Actuator in Action

6.1.2. Instrumentation

The instrumentation for this research was designed and analyzed by Julia Sargent

(2019). A detailed understanding of the process is discussed in her thesis. To summarize, Figure

6.4 demonstrates the layout of all components of the instrumentation. The load cell (not shown)

recorded the load being applied by the hydraulic jack. The main lateral deflection was

documented using two devices: a string potentiometer (string pot) (7) to record the larger

displacements, and a linear potentiometer (lpot) (8) to record the initial smaller displacements

and calibrate the string pot. There were six other string pots (1, 2, 3, 4, 5, 6) positioned on one

face of the wall to track panel deformation and eventually help determine the failure

mechanism. Two lpots were used to register any slipping that could occur between the wall and

the foundation (10) or the wall and the top beam (9). Finally, two lpots (11, 12) were used to

report any uplift that could occur due to rocking.
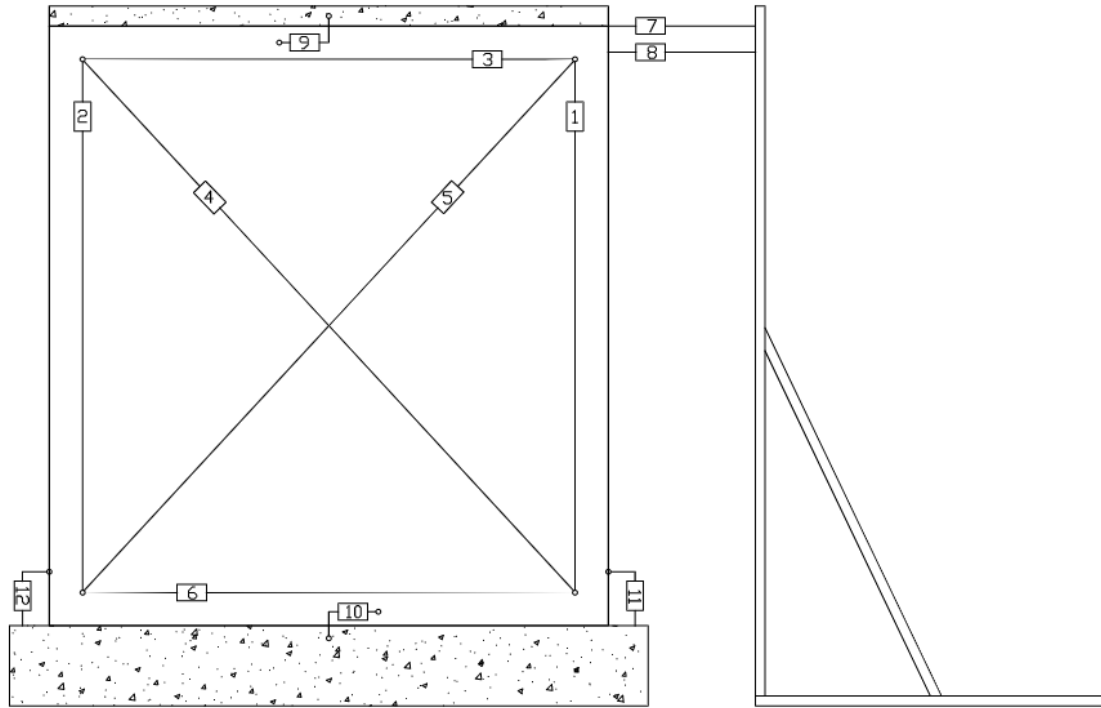
Figure 6.4: CAD of Instrumentation Layout

6.1.3. *Photography Tracking*

After the wall was constructed and completely dried, a thin plaster layer was mixed and applied on the "viewing" side of the wall, opposite the instrumentation setup side. The plaster layer was a mixture of the clay subsoil and water. The purpose of this layer was to provide a "clean surface" with no visible construction cracks, to enable any cracks as a result of the testing to be easily seen. Figure 6.5 illustrates the plaster layer being applied to the viewing face.

Throughout the entire testing, a camera was set up to take pictures every 5 seconds of the "viewing" face. This allowed a visual representation of the creation and expansion of cracks on the wall to be captured, potentially aiding the analysis of the collected data.

Figure 6.5: Thin Plaster Layer Applied to Wall

6.1.4. Loading Protocol

The requested cyclic loading progression for all the walls can be seen in Table 6.1, which was displacement-controlled. The protocol defines a cycle as the requested displacement being reached in both the positive and negative directions. Each displacement experienced two full cycles before moving on to the next displacement, as seen in Figure 6.6. For this testing, a positive displacement meant the wall was being pulled and a negative displacement meant the wall was being pushed. This was due to the loading frame and the displacement frame being on opposite ends of the wall, as seen in Figure 6.2. This process was continued until the specimen experienced failure which is defined as the strength being to 80% of the maximum strength. Voon (2007) chose this protocol for two specific reasons:

- The displacement readings were the only controlling factor used to decrease the dependency on other instrument readings, such as load that can vary.

- The smaller initial displacements were utilized to avoid failure being reached at an early stage of the testing.

Table 6.1: Cyclic Loading Sequence

Cycle	Imposed Displacement (in)	% Drift
1-2	0.05	0.054%
3-4	0.1	0.108%
5-6	0.2	0.215%
7-8	0.3	0.323%
9-10	0.5	0.538%
11-12	0.75	0.806%
13-14	1	1.075%
15-16	1.5	1.613%
17-18	2	2.151%
19-20	3	3.226%
21-22	4	4.301%
23-24	5	5.376%
25-26	6	6.452%
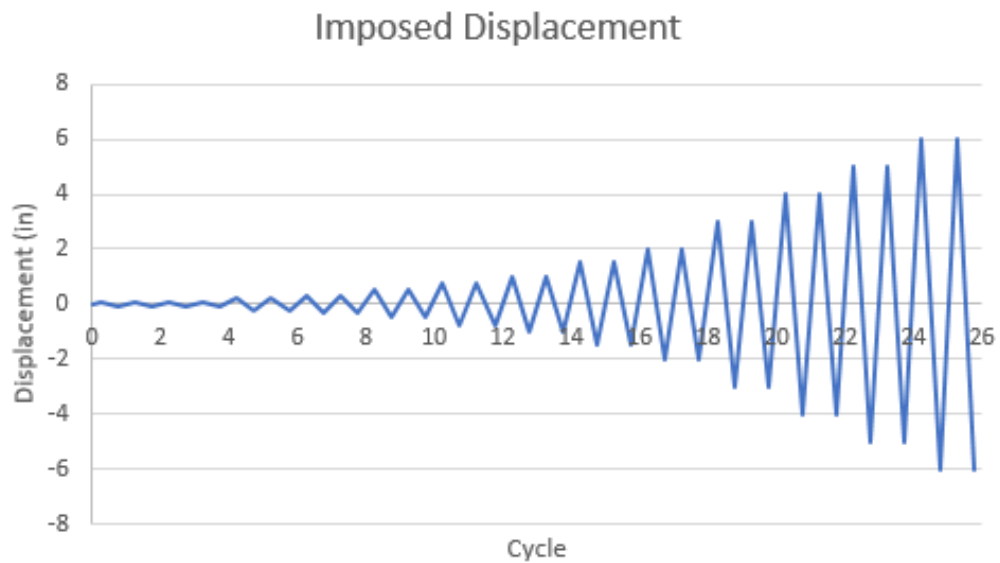
Figure 6.6: Imposed Displacement History

6.2. Wall Details and Testing

Figure 6.7 represents the completed cob wall with steel pipe reinforcement. The wall was constructed following the procedure outline in chapter 4. Table 6.2 illustrates the wall dimensions after it was able to completely dry. The varying dimensions for the same component could be a result of shrinkage.

Figure 6.7: Pipe Stem Wall before Testing

Table 6.2: Dimensions of the Steel Pipe Reinforced Cob Wall

Pipe Reinforcing				
	L	**W**		**H**
Bottom	7.38	14.00	Right Side	7.44
Middle	7.25	14.00	Middle	7.52
Top	7.25	13.50	Left Side	7.48
Average	**7.29**	**13.83**		**7.48**

Figure 6.8 displays the real displacement history applied to the wall. Compared to Figure

6.6, the cycles correlating to ±0.4 inches of displacement were skipped since no signs of early-

stage failure were present. The plateau seen just after 100 minutes represents the time when

the string pots were removed from the wall to avoid damaging the instruments. For the last two

cycles, the wall was only *pulled* to the displacements of 5 inches due to wall torsion that was

noticed on the push cycles.
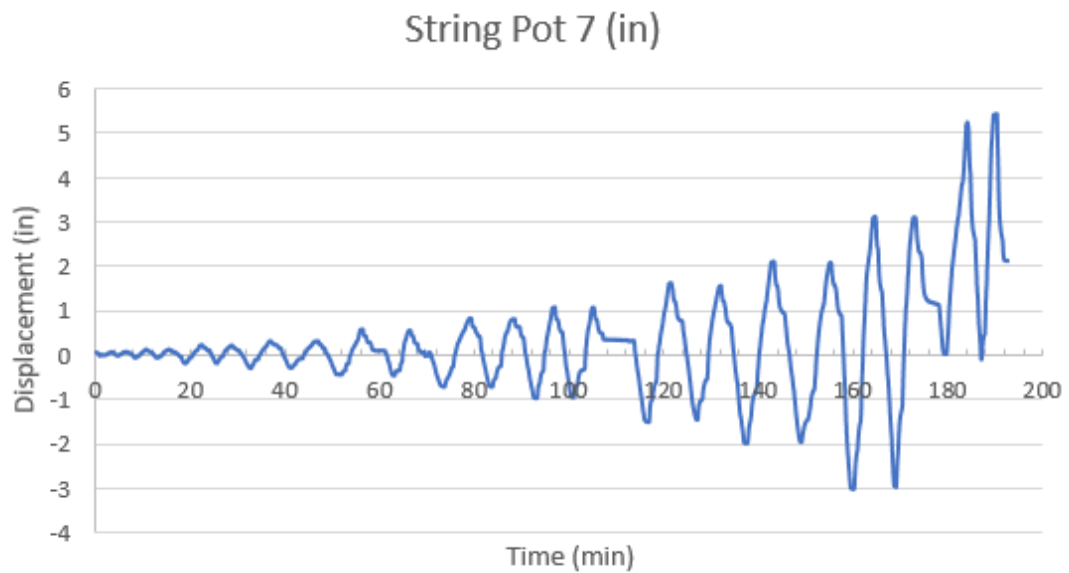
Figure 6.8: Actual Displacement History

As discussed in 6.1.2, there were two instruments measuring the lateral displacement.

The string pot was used to measure the displacement of the entire test but due to the noisy

curves it created, an lpot was used to measure those initial smaller displacements. Figure 6.9

compares the curves created from the two instruments. The string pot data was adjusted to try

to match the lpot so that the entire string pot data was more accurate.
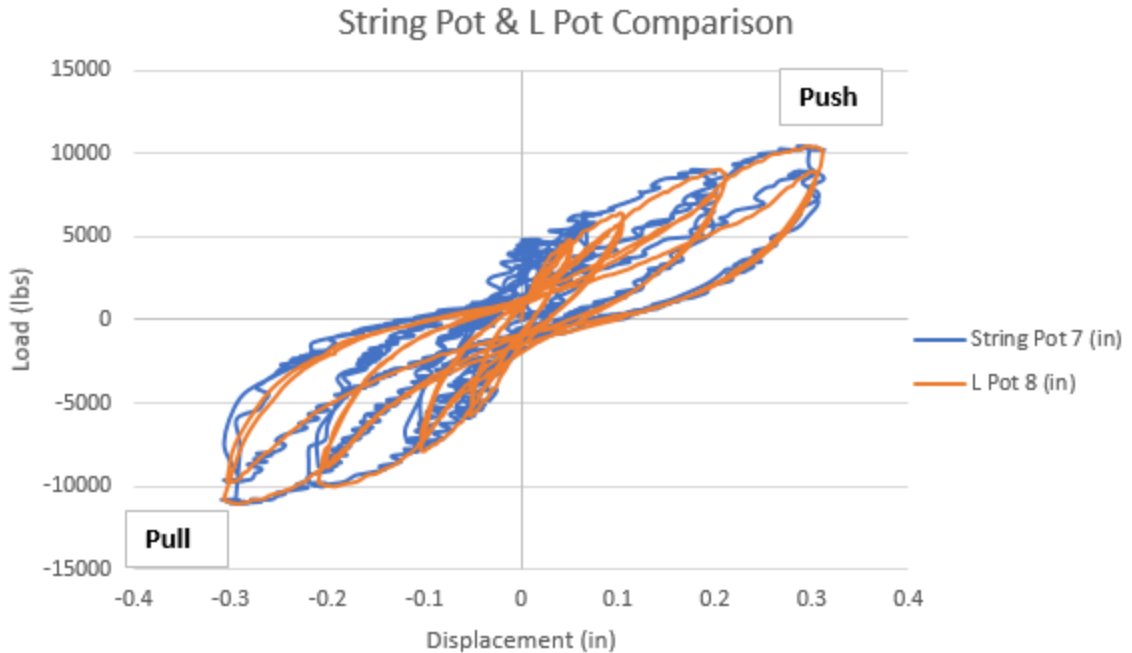
Figure 6.9: Comparison of Displacement Instruments

The wall was tested on March 19, 2019 at Quail Spring Permaculture. The testing

continued until the strength of the wall dropped below 80% of the maximum load during the

22nd cycle. This ultimate displacement occurred at 5.35 inches in the pull direction only.

Maximum strength emerged around 25,000 lbs in the pull direction and 20,000 lbs in the push

direction during the 21st cycle. During the 21st cycle, the load peaked and then plateaued until

failure during the next cycle. The hysteresis for this test can be seen in Figure 6.10, and a

summary table of the results is shown in Table 6.3. This test concluded after failure occurred

due to the foundation failure. Figure 6.11 demonstrates the pipe reinforcement in the

foundation failure.
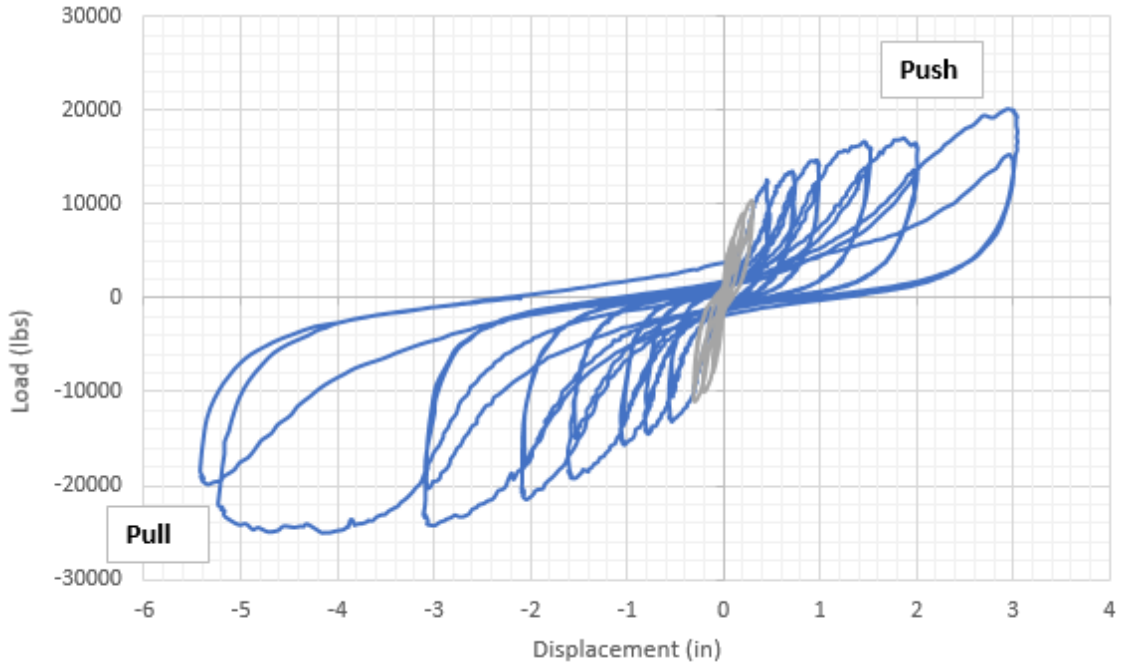
Figure 6.10: Force-Displacement Hysteresis

Table 6.3: Results from In-Plane Cyclic Testing

TEST RESULTS					
Loading Direction	V_{max} (lb)	δ_{Vmax}		δ_u	
		(in)	(% drift)	(in)	(% drift)
Push (+)	20078.2	2.942	3.163%	-	-
Pull (-)	-24972.9	4.168	4.482%	5.346	5.748%

Figure 6.11: Foundation at Failure

Using the photography tracking, initial cracking and growth throughout testing was able to be recorded. The first set of cracks formed from the test seemed to occur during the 9th cycle out to 0.5 inches and have been emphasized in Figure 6.12. The cracking right before failure can be seen in Figure 6.13. Further investigation of these cracks transpires in chapter 7.

Figure 6.12: Wall Cracks at 0.5 inch Displacement

Figure 6.13: Wall Cracks at Failure

7.   RESULTS AND ANALYSIS

This chapter examines the data found in chapter 6 and discusses the results. Wall deformations from the instrumentations, photography tracking, and a backbone curve aid in determining the failure mode. Yielding points are determined with multiple methods and used to establish R-Factor values.

7.1.   Wall Properties

Immediately following testing, samples were drilled from the cob wall with pipe reinforcing. These samples were taken from multiple locations on the wall and tested for moisture content. The values can be seen in Table 7.1 and are compared to the moisture contents of the blocks that underwent testing on campus, Table 3.7. The moisture contents for the full-scale wall mimicked the values from the blocks, meaning the wall should display similar strengths to the blocks.

Table 7.1: Moisture Content of Cob in Pipe Reinforcing Wall

WALL 3 (PIPE STEM) MOISTURE CONTENT						
Date Sampled		3/20/2019, 12:55 pm				
Weighed and Placed in Oven		3/21/2019, 10:30 am				
Oven Dry Measured		3/22/2019, 1:15 pm				
Sample	1	2	5	6	7	8
Dish ID	8	34	98	203	229	233
Mass Dish (g)	30.58	30.85	30.74	30.30	30.24	29.86
Mass Dish + Sample (g)	73.61	89.41	75.24	61.23	72.31	97.43
Oven Dry						
Mass Dish + OD (g)	72.95	88.54	74.56	60.76	71.60	96.61
Moisture Content (%)	1.6%	1.5%	1.6%	1.5%	1.7%	1.2%
3/25/2019, 5:50 pm						
Mass Dish + Sample (g)	73.20	88.88	74.81	60.91	71.84	96.99
Moisture Content (%)	0.6%	0.6%	0.6%	0.5%	0.6%	0.6%
3/27/2019, 1:40 pm						
Mass Dish + Sample (g)	73.27	88.96	74.89	60.96	71.90	97.07
Moisture Content (%)	0.8%	0.7%	0.8%	0.7%	0.7%	0.7%
3/28/2019, 11:15 am						
Mass Dish + Sample (g)	73.26	88.95	74.88	60.95	71.89	97.08
Moisture Content (%)	0.7%	0.7%	0.7%	0.6%	0.7%	0.7%
Oven Dry 3/29/2019, 1:20 pm						
Mass Dish + Sample (g)	72.84	88.41	74.47	60.72	71.51	96.42
Moisture Content (%)	1.8%	1.7%	1.8%	1.7%	1.9%	1.5%
Oven Dry 4/2/2019, 11:30 am						
Mass Dish + Sample (g)	72.81	88.36	74.43	60.68	71.47	96.37
Moisture Content (%)	1.9%	1.8%	1.9%	1.8%	2.0%	1.6%

7.2. General Shear Behavior

The following section describes the shear characteristics utilizing the backbone curve, displacement components, and behavioral characteristics.

7.2.1. Backbone Curve

The backbone curve in Figure 7.1 was created by analyzing the data from the hysteresis in Figure 6.10. The backbone curve is an envelope of the maximum loads reached at each defined displacement. The backbone curve symbolizes the ductility of the material. A more ductile material can continue to resist additional load after the yielding point is reached, where a brittle material will fracture relatively close to its yielding point. The yielding point for this material can slightly be seen when the curve starts to flatten. This could be a result of the cob cracking and the activation of the straw and steel reinforcement. The curve continued to increase until about 2 inches (in the pull direction), where the slope of the curve noticeably decreased and appeared to plateau before reaching a maximum load. This plateau is a characteristic of a ductile failure.
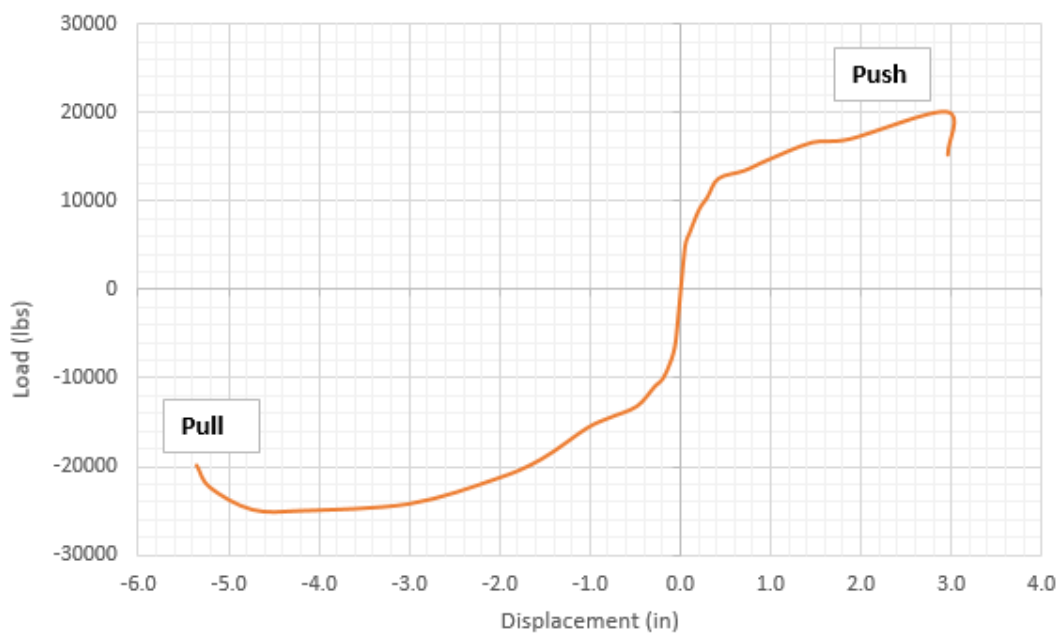
Figure 7.1: Backbone Curve

7.2.2. Displacement Components

From Figure 6.4, there are six string pots on the face of the wall that measure panel deformations: two measure vertical displacement, two measure horizontal displacement, and two measure for diagonal displacement. These displacements were able to be converted into shear, flexural, and rocking components from each wall's total displacement. Full derivations of the component equations can be found in Appendix C of Voon (2007). Adjusted equations to match these variables in Figure 6.4 are displayed below:

$$u_s = \frac{d}{2L}(\delta_4 - \delta_5) - \frac{h^2}{6(2d_u+h)}\frac{(\delta_1-\delta_2)}{L} \tag{Eq. 7.1}$$

$$u_b = \frac{(\delta_1-\delta_2)}{L}\left[h\frac{d_u+\frac{2h}{3}}{2d_u+h} + d_u\right] \tag{Eq. 7.2}$$

where d is the length of the diagonal string pots

d_u is the vertical distance form string pot 3 to applied load

L is the horizontal distance between string pots 1 and 2

h is the vertical distance between string pots 3 and 6

From Figure 6.4, there are two lpots on the edges of the wall that measure rocking. The adjusted equation for rocking can been evaluated:

$$u_r = \frac{d_{11}-d_{12}}{L_w+2l_s}h_e \tag{Eq. 7.3}$$

where L_w is the horizontal length between string pots 1 and 2

l_s is the horizontal length from the wall and string pot 11 (or 12)

h_e is the vertical length between the foundation and top beam

These components each contribute to the overall total displacement. Figures 7.2 represents each component displacement relative to the total displacement. Figure 7.3 demonstrates how each component contributes to the overall hysteresis curve. Both these figures conclude a shear failure mode of the pipe reinforcing wall.

64
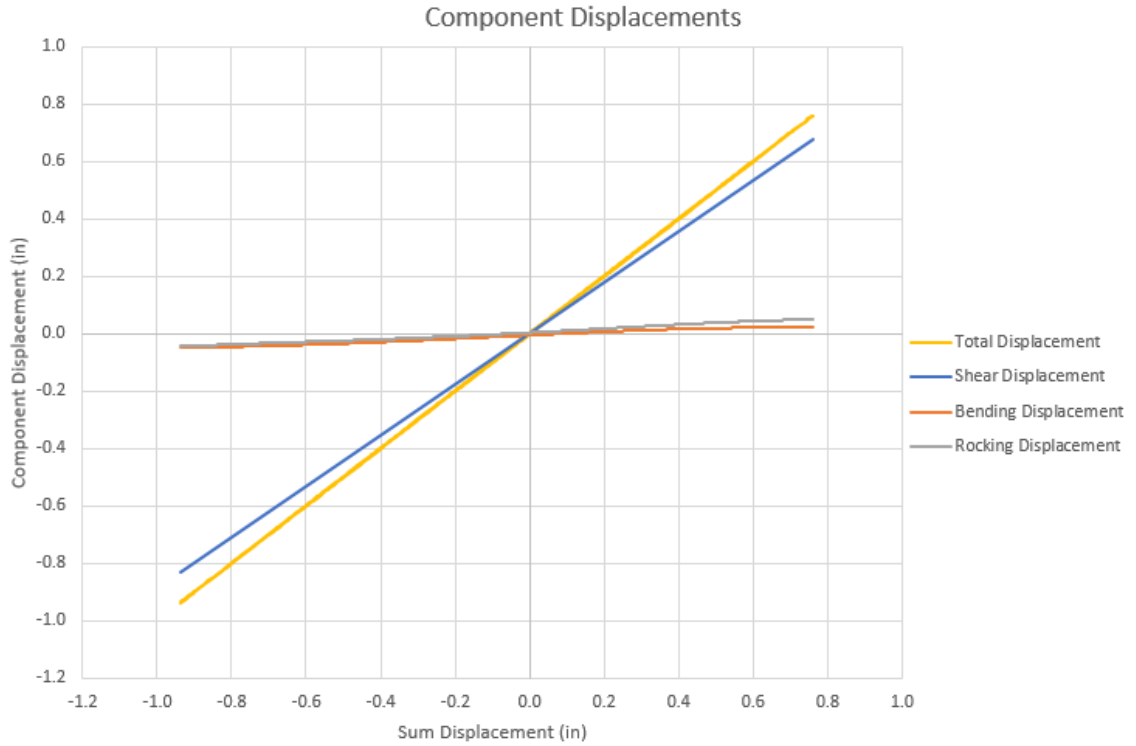
Figure 7.2: Displacement Components with Respect to Sum
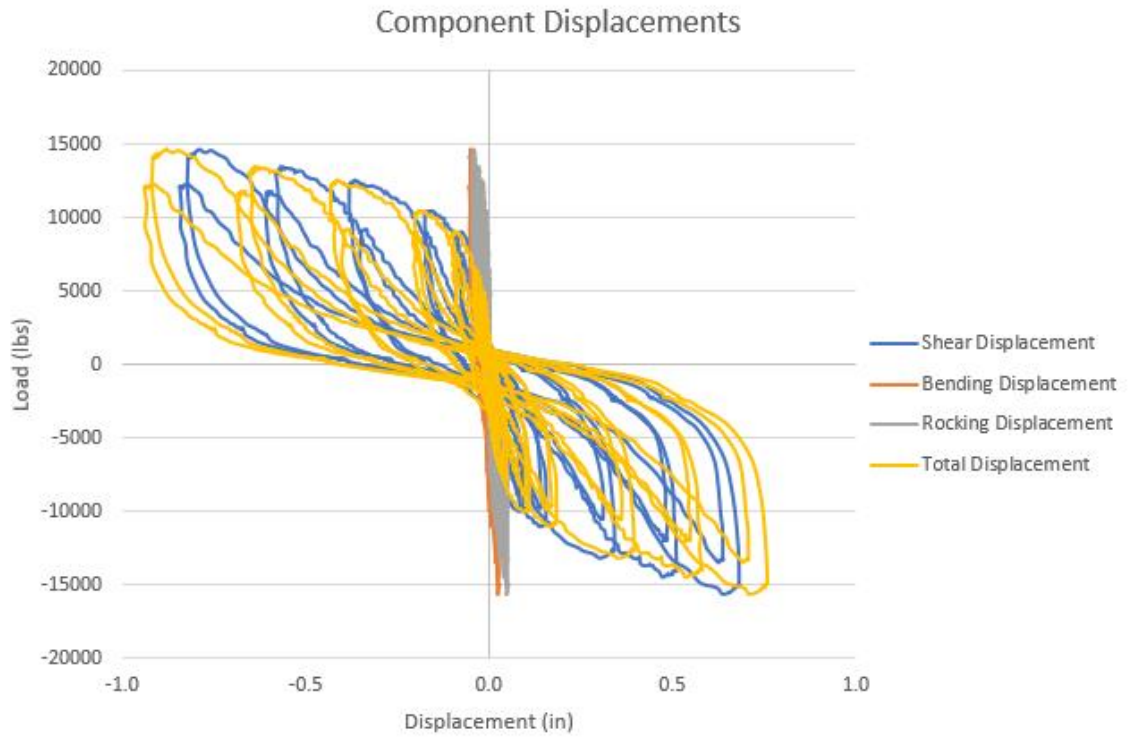
Figure 7.3: Displacement Components' Hysteresis Curve

7.2.3. Behavioral Characteristics

Images of the wall and cracks formed were captured throughout the entirety of testing. These cracks allowed visual assessments to be made about the behavior of the wall. The cracks can indicate failures in bending and shear, as shown in Figure 7.3. Cracks as a result of bending generate horizontal cracks, where cracks from shear generate diagonal cracks.
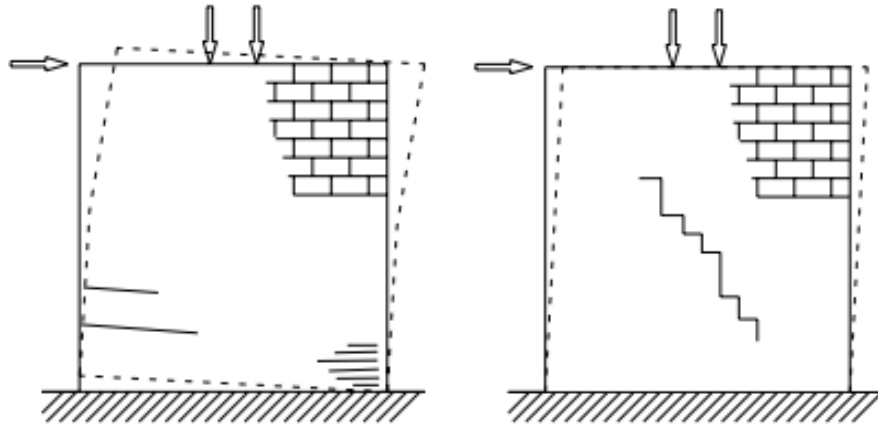
Figure 7.4: Cracking of Flexural Failure (left) and Shear Failure (right)

The pipe stem wall displayed behavioral characteristics like those observed in the cob only and double mesh walls. The earlier loading displacements produced diagonal cracks resembling a shear failure. As the applied displacements increased, the foundation developed cracks from the friction with the loading beam. After completion of testing, the pattern created from the cracks was reflective of brittle shear failure, as seen in Figure 7.4, which could be a result of the failure of the cob and the activation of the straw and pipes.

(a) Brittle shear failure   (b) Ductile shear failure
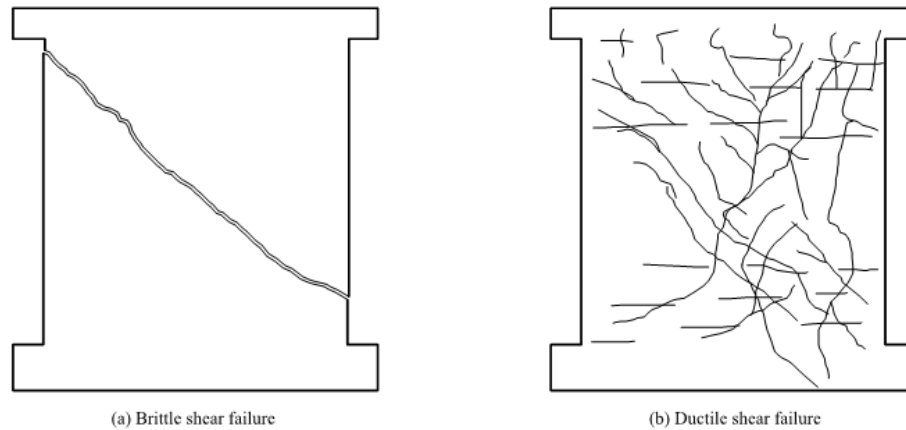
Figure 7.5: Failure Mode Cracks from Voon (2007)

From the testing, it was observed that the wall continued to increase in strength. Some horizontal cracks were noticed on the face of the wall and appeared to occur where lifts were completed. This leads to the outcome that the lifts were not fully connected from the thumbing process and therefore were considered a weak point. Finally, the cracks formed prior to failure indicate a ductile shear failure which is agrees with the outcomes discussed from prior methods.

7.3. Yielding Methods

This section describes the two methods utilized to determine the yield points for the backbone curve in Figure 7.1.

7.3.1. *Trendline Method*

The first method for determining the yield point was the Trendline Method conducted in the Santa Clara University Reports (2018). This method resulted in two yield points, one in each direction. This method consisted of the following steps:

1. Set the datum as the first point of the hysteresis curve corresponding to the first max load and its displacement achieved during the first cycle

2. Graph the datum and the next point on the hysteresis

3. Add a trendline, choose a linear fit, and display the R-squared value

4. If the R-squared value is greater than 0.9, include the next point on the hysteresis in

your data and complete steps 2 and 3 again.

*The yield point is defined as the last point added to the trendline to maintain an R-squared

value greater than 0.9.

The yielding points found from this method are shown in Figure 7.4 with their respective

R-squared values.
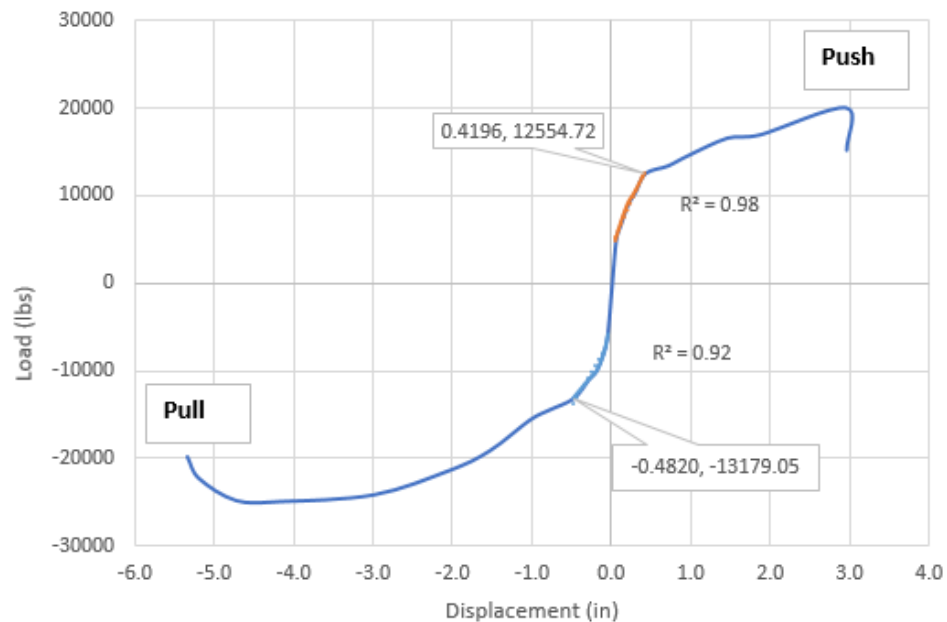
Figure 7.6: Trend line Yield Point Method

7.3.2. Furthest Point Method

The second method for determining a yield point was the Furthest Point Method

recommended from Dr. Qu, who had used this method in prior research. The steps for this

method include the following:

1. Draw a line connecting the max load and its respective displacement to the origin (0,0).

   a. Determine the length of the line and angle to the positive displacement axis

2. Draw a line a point from the origin

   a. Determine the length of the line and angle to the positive displacement axis

3. Calculate the internal angle between the line from 2 and the line from 1

4. Multiply the internal angle by the length of the line from 2 to derive the distance of the point to the max load line

5. Repeat steps 2-4 for each point on the backbone curve

*The yield point is defined as the point furthest from the max load line.

The yield points from this method are shown in Figure 7.5 with their respective lengths.
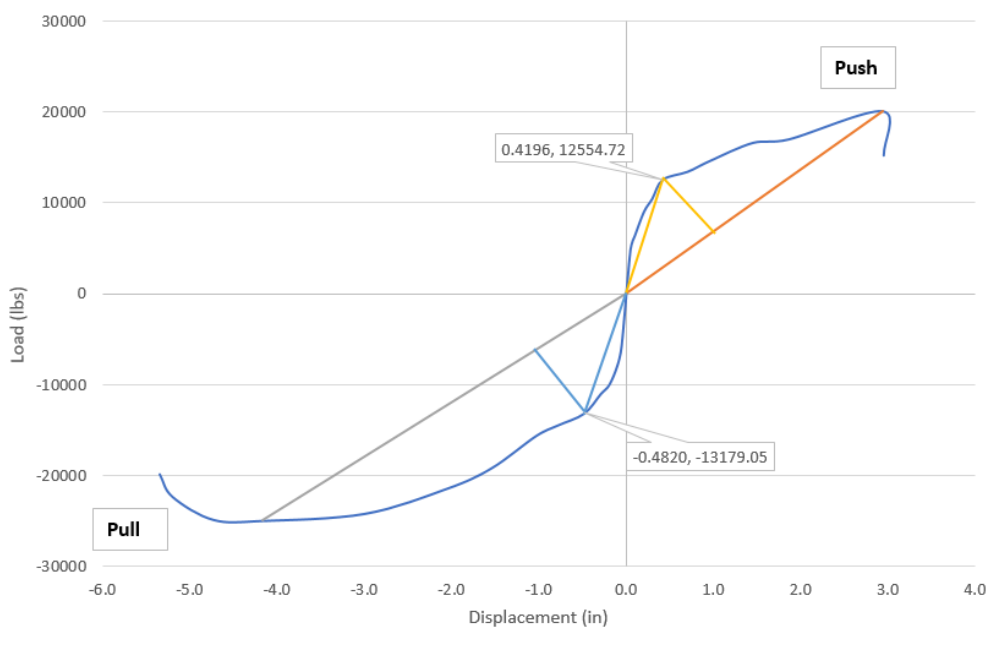
Figure 7.7: Furthest Point Yielding Method

The two methods computed the same values for yielding points, seen in Table 7.2.

Table 7.2: Summary of Yield Points

EXPERIMENTAL YIELD POINTS FOR COB			
Yield Method	Direction	Yield Point	
		Load (lb)	Displacement (in)
Trendline	Push	12555	0.420
	Pull	13179	0.482
Furthest Point	Push	12555	0.420
	Pull	13179	0.482

7.4. Seismic Response Modification Factor, R-Factor

From Chopra's "Dynamics of Structures" chapter 7 and the APA Report 158, the method for calculating the R-Factor is summarized below in Equation 7.4. Since both yielding methods resulted in the same yield point, only one R-Factor was found for each direction. A summary of the R-Factor values is shown in Table 7.3.

$$R = R_\Omega R_d \qquad \text{(Eq. 7.4)}$$

$$\text{where} \quad R_\Omega = \Omega = \frac{P_{max}}{P_{design}} \text{(assumed 1 for this research)}$$

$$R_d = \sqrt{2\mu - 1}$$

$$\mu = \frac{\Delta_u}{\Delta_y}$$

Table 7.3: Summary of R-Factors

R-FACTORS FOR COB	
Direction	R Factor
Push	3.5
Pull	4.5

7.5. In-Plane Stiffness

The in-plane stiffness of the pipe stem wall was determined using two methods: theoretical and experimental. For the theoretical method, the stiffness was estimated as a combination of the cob wall acting as a cantilever and the pipe reinforcement acting as a moment frame. Each component is comprised of flexural and shear stiffness. The theoretical stiffness is calculated as follows:

$$K_{m,cob} = \frac{3E_{cob}I_{cob}}{h^3} \qquad \text{(Eq. 7.5)}$$

$$K_{m,steel} = 3 * \frac{12E_{steel}I_{steel}}{h^3} \qquad \text{(Eq. 7.6)}$$

$$K_{v,cob} = \frac{A_{cob}G_{cob}}{L} \qquad \text{(Eq. 7.7)}$$

$$K_{v,steel} = \frac{A_{steel}E_{steel}}{L} \qquad \text{(Eq. 7.8)}$$

where E is the modulus of elasticity of each material

I is the moment of inertia of each material

A is the area of each material

$$G_{cob} = \frac{E}{2(1+v)}$$

$$v = \frac{-\varepsilon_{transverse}}{\varepsilon_{longitudinal}}$$

Since the steel columns and beams act concurrent to the cob wall, the total stiffness can be calculated as:

$$K_m = K_{m,cob} + K_{m,steel} \qquad \text{(Eq. 7.9)}$$

$$K_v = K_{v,cob} + K_{v,steel} \qquad \text{(Eq. 7.10)}$$

$$K_{tot} = \frac{1}{\frac{1}{K_m}+\frac{1}{K_v}} \qquad \text{(Eq. 7.11)}$$

Using equations 7.5 thru 7.8, the theoretical stiffness of each component can be found. These stiffnesses are summarized in Table 7.4 for Cob and Table 7.5 for the Reinforcing Steel.

Table 7.4: Theoretical Stiffness from Cob

THEORETICAL STIFFNESS FROM COB		
Variable	Value	Unit
E	39,400	psi
G	18,425	psi
I	718,293	in^4
A	1,206	in^2
k_m	116,931	lb/in
k_v	247,264	lb/in
k_{tot}	79,388	lb/in

Table 7.5: Theoretical Stiffness from Steel

THEORETICAL STIFFNESS FROM STEEL		
Variable	Value	Unit
E	180,560	psi
E_m	180,560	psi
E_v	180,560	psi
I	6.525	in^4
A	2.930	in^2
k_m	58	lb/in
k_v	6,131	lb/in
k_{tot}	58	lb/in

Using equations 7.9 thru 7.11, the total theoretical stiffness of the system is summarized

in Table 7.6.

Table 7.6: Total Theoretical Stiffness

TOTAL THEORETICAL STIFFNESS		
Variable	Value	Unit
k_m	116989.50	lb/in
k_v	253394.74	lb/in
k_{tot}	80037.22	lb/in

The experimental in-plane stiffness is considered linear in the earlier stages of the test.

Therefore, according to Hooke's Law, the relationship between load and displacement is:

$$F = Ku \qquad \text{(Eq. 7.12)}$$

Thus, the experimental stiffness is equivalent to the slope of the load-deflection curve

while the material behaves elastically. Figure 7.6 includes the initial cycles considered to be

elastic. Cycles were added to this close-up analysis as long as the linear regression line

maintained an R value greater than 0.85. The slope of this linear regression line represent the

experimental stiffness. Comparing the experimental and theoretical values determines a phi

value that can be used to reduce design strengths appropriately, per this research.

$y = 64952x - 138.49$
$R^2 = 0.8608$
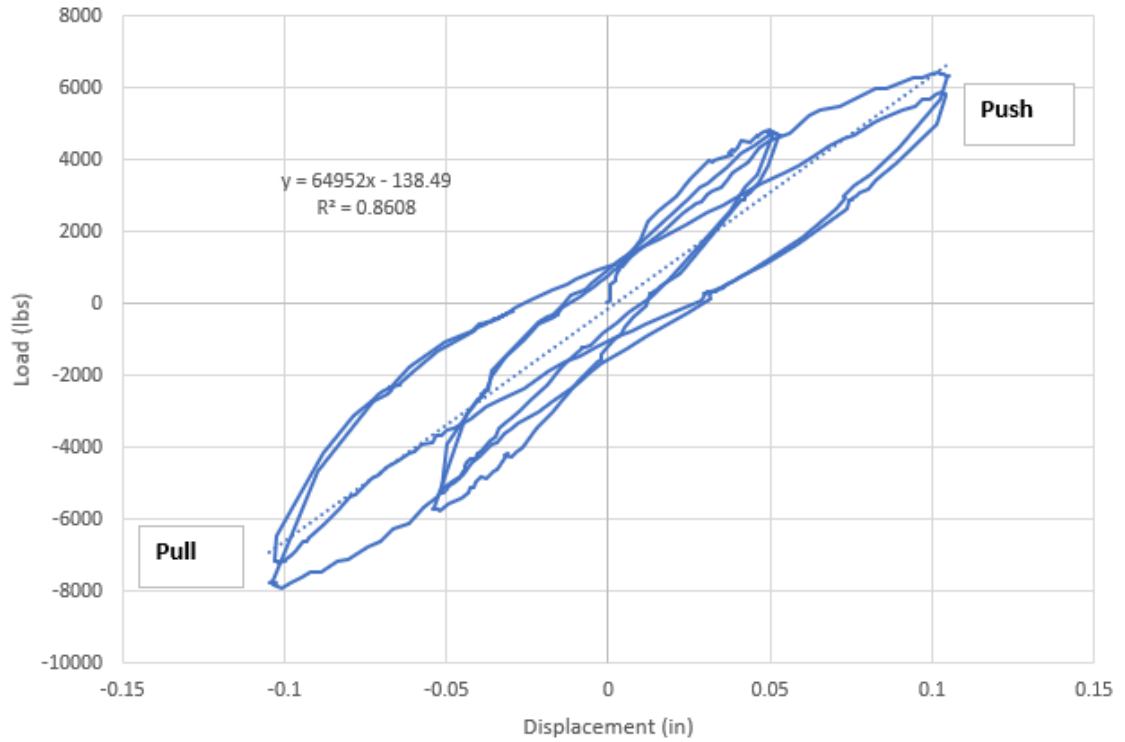
Figure 7.8: Experimental Stiffness

Table 7.7: Comparison of Experimental and Theoretical Stiffness

EXPERIMENTAL STIFFNESS FOR COB	
Method	k (lb/in)
Experimental	64952
Theoretical	80037
phi	0.81

8.   CONCLUSION AND FUTURE RESEARCH

With the reemergence of cob as a building material, there is interest in the material

properties and structural integrity of it. Due to the lack of current information, there are no

specific codes or standards set which is preventing the construction with cob to occur. This

research focused on full-scale in-plane cyclic testing of cob walls with varying reinforcement.

This report specifically discussed the results of the pipe stem wall. The failure modes were

determined by analyzing the panel deformation and behavioral characteristics of the wall. A

maximum load of the wall was found and a seismic response modification factor was computed.

8.1.   Conclusion

8.1.1.   Materials

- The clay subsoil used in the cob mixture was classified as a Moist Tan Lean Clay with

  Gravel.

- 17 rectangular prisms that underwent the modulus of rupture test resulted in a flexural

  strength of 33.05 psi. This value was within the range found in prior research.

- A unit weight of 107.3 pcf was found.

- Compressive strength, Young's modulus, and moisture content were calculated as 174

  psi, 39,369 psi, and 1.6%, respectively.

8.1.2.   In-Plane Shear Testing

- The pipe stem wall experienced a peak load of about 25,000 lbs at a 4.168 inch

  displacement.

- The ultimate point was reached when the strength dropped to 80% of the maximum

  load. Ultimate occurred at a 5.346 inch displacement where failure also transpired.

- Failure of this wall was a result of the reinforcement in the foundation popping out of

  the foundation and further testing of the wall being prevented.

- The backbone curve, deformation components, and behavior characteristics concluded a ductile shear failure. The plateau in the backbone curve and the final cracks present on the surface of the wall demonstrated ductility, where the deformation components exhibited high shear contributions with minimal bending and rocking components.

- Two separate methods were used to calculate a yield point of 12,555 lbs and 0.420 inch displacement in the push direction, and 13,200 lbs and 0.482 inch displacement in the pull direction.

- The analysis of this test resulted in R-Factors of 3.5 (short period) and 7 (long period) in the push direction and 4.5 (short period) and 11 (long period) in the pull direction.

- Stiffness was found to be about 30,000 lb/in experimentally and 65,000 lb/in theoretically, resulting in a phi value of 0.42.

8.2. Recommendations for Future Work

- Future research should include the effects of straw on the strength of full-scale walls. There is current research demonstrating the effects of straw on smaller blocks for compressive and flexure strengths, but their results appeared skewed due to the cramped area of application. For this test, straw quantity was not recorded and therefore could not be considered in analysis.

- Successful testing of full-scale cob only walls would be beneficial, so that comparisons could be made for slightly altered walls.

- This pipe stem wall consisted of additional vertical reinforcement. The contribution of different reinforcing layouts such as the addition of horizontal reinforcement or diagonal bracing. Overall, a limit to the amount of reinforcement that can be added before there is no longer a significant increase in the shear strength should be determined.

- Additional iterations of this wall with similar construction techniques should be tested to verify the values obtained in this research.

- Iterations of the varying cob mixtures and their effects on strength should be tested to verify the best combination to use when building with cob.

- Similar reinforcement to this wall should be tested again with improved foundation reinforcement so that the capacity of the cob wall itself can be determined.

REFERENCES

Akinkurolere, O. O., et al. "Engineering Properties of Cob as a Building Material." *Journal of Applied Sciences 6 (8): 1882-1885, 2006*, pp. 1882–1885.

ASTM International. *Standard Practice for Classification of Soils for Engineering Purposes (Unified Soil Classification System)* (D2487-17). West Conshohocken, PA: ASTM International, 2017. doi: https://doi.org/10.1520/D2487-17.

ASTM International. *Standard Specification for Steel Wire and Welded Wire Reinforcement, Plain and Deformed, for Concrete* (A1064/A1064M-10). West Conshohocken, PA: ASTM International, 2010. doi: https://doi.org/10.1520/A1064_A1064M-10E01.

ASTM International. *Standard Test Method for Compressive Strength of Cylindrical Concrete Specimens* (C39/C39M-18). West Conshohocken, PA: ASTM International, 2018. doi: https://doi.org/10.1520/C0039_C0039M-18.

ASTM International. *Standard Test Method for Flexural Strength of Concrete (Using Simple Beam with Center-Point Loading)* (C293/C293M-16). West Conshohocken, PA: ASTM International, 2016. doi: https://doi.org/10.1520/C0293_C0293M-16.

ASTM International. *Standard Test Method for Particle-Size Analysis of Soils* (D422-63[2007]E2). West Conshohocken, PA: ASTM International, 2007.

ASTM International. *Standard Test Methods for Liquid Limit, Plastic Limit, and Plasticity Index of Soils* (D4318-17E1). West Conshohocken, PA: ASTM International, 2017. doi: https://doi.org/10.1520/D4318-17E01.

ASTM International. *Standard Test Methods for Specific Gravity of Soil Solids by Water Pycnometer* (D854-00). West Conshohocken, PA: ASTM International, 2000. doi: https://doi.org/10.1520/D0854-00.

Brunello, Gabi, et al. "Cob Property Analysis," *Santa Clara University,* 2018.

Eberhard, Daniel, et al. "Cob: A Sustainable Building Material," *Santa Clara University, 2018.*

Google. [Satellite maps of Ventucopa, CA and Quail Springs Permaculture]. *Google Maps.*

    Retrieved from maps.google.com, 2019.

Goshey, Oliver. "Cob: Getting to Know One of Construction's Most Ancient and Versatile

    Materials." *Abundant Edge,* Abundant Edge, 27 May 2016,

    www.abundantedge.com/articles-1/2016/5/24/cob-getting-to-know-one-of-

    constructions-most-ancient-and-versatile-materials

Holtz, R. D., et al. *An Introduction to Geotechnical Engineering*. 2nd ed., Pearson, 2011.

Lehmwellerbau, Ziegert C. "Konstruktion, Schaden und Sanierung, Berichte aus dem

    Konstruktiven Ingenieurbau," *Technical University of Berlin,* 2003.

Miccoli, Lorenzo, et al. "Mechanical Behaviour of Earthen Materials: a Comparison between

    Earth Block Masonry, Rammed Earth and Cob." *Construction and Building Materials*, Vol.

    61, 30 June 2014.

Pullen, Quinn M., and Todd V. Scholz. "Index and Engineering Properties of Oregon

    Cob." *Journal of Green Building*, 2009, pp. 88–106.

Qu, Dr. Bing. "Furthest Point Method." *California Polytechnic State University,* Interview, 2019.

Rizza, Michael Scoles, and Hana Mori Bottger. "Effect of Straw Length and Quantity on

    Mechanical Properties of Cob," *University of San Francisco,* 2013.

Sargent, Julia. "In-Plane Cyclic Testing of a Reinforced Cob Wall." *California Polytechnic State*

    University, 2019.

Saxton, R. H. "The Performance of Cob as a Building Material," *The Structural Engineer,* Vol. 73,

    No. 7, 1995, pp. 111–115.

Smith, Michael. "The History of Cob." *NetWorks Productions*,

    www.networkearth.org/naturalbuilding/history.html.

Snell, Clarke, and Tim Callahan. *Building Green*. 2nd ed., Lark Books, A Division of

    Sterling Publishing Co., Inc, 2009.

Voon, Kok Choon. "In-Plane Seismic Design of Concrete Masonry Structures." *University of*

    Auckland, 2007, http://hdl.handle.net/2292/580.

Weismann, Adam, and Katy Bryce. *Building with Cob: A Step-by-Step Guide*. Green Books, 2006.

APPENDICES

APPENDIX A. SAND AND SOIL PROPERTIES

A.1. Particle-Size Analysis

DEPARTMENT OF CIVIL AND ENVIRONMENTAL ENGINEERING

Hydrometer Analysis

Test Method: ASTM D422, D2487

Project Name	Quail Springs Cobb Wall Testing	Project No.	--
Tested By	GVP-LEB	Testing Date	11/29/2018

SPECIMEN ID AND CLASSIFICATION					
Boring No.	--	Sample No.	--	Depth (ft)	--
Soil Description	Lean CLAY with sand and gravel (CL): tan, moist				

GRAVEL GRADING					
Tray ID	B-13	Air-Dry Soil Mass (g)	556.92	Corrected Dry Mass (g)	542.76

Sieve No.	Size, mm	Mass Retained (g)	Cumulative Retained (g)	% Retained	Combineed % Passing
3 in	76.2	0.00	0.00	0.0%	100.0%
2 in *	50.8	0.00	0.00	0.0%	100.0%
1 in *	25.4	0.00	0.00	0.0%	100.0%
3/4 in *	19.1	0.00	0.00	0.0%	100.0%
1/2 in *	12.7	14.90	14.90	2.7%	97.3%
3/8 in *	9.50	25.81	40.71	7.5%	92.5%
No. 4 *	4.75	83.64	124.35	22.9%	77.1%
Pan		432.37	556.72	Sieve Continuity	100.0%

WATER CONTENT OF MINUS #4 =			2.6%	#4 BY #10 GRADING	
Dish ID	ST-108	Moist Soil + Dish (g)	238.36	Mass of Air-Dried Soil (g)	223.28
Dish Mass (g)	128.21	Dry Soil + Dish (g)	235.56	Corrected Dry Mass (g)	217.60

Sieve No.	Size, mm	Mass Retained (g)	% Retained	% Passing	Combineed % Passing
No. 10	2.00	41.48	19.1%	80.9%	62.4%
Pan		181.80	Split Minus #10 for Hydrometer Test (152H)		

Post Wash ID	ST-51	Dry Mass Post Wash (g)	10.53	#16 BY #200 GRADING	
Sieve No.	Size, mm	Mass Retained (g)	Cum. Ret. (g)	% Retained	% Passing	Combined % Passing
No. 16	1.180	0.33	0.33	0.4%	99.6%	62.1%
No. 30	0.600	0.58	0.91	1.2%	98.8%	61.6%
No. 50	0.300	1.19	2.10	2.8%	97.2%	60.7%
No. 100	0.150	2.30	4.40	5.9%	94.1%	58.7%
No. 200	0.075	5.46	9.86	13.1%	86.9%	54.2%
Pan		0.59	10.45	Sieve Continuity	100.8%

HYDROSCOPIC WATER CONTENT =	2.3%	HYDROMETER

80

DEPARTMENT OF CIVIL AND ENVIRONMENTAL ENGINEERING

Hydrometer Analysis

Test Method: ASTM D422, D2487

Project Name	Quail Springs Cobb Wall Testing	Project No.	--
Tested By	GVP-LEB	Testing Date	11/29/2018

SPECIMEN ID AND CLASSIFICATION						
Boring No.	--		Sample No.	--	Depth (ft)	--
Soil Description	Lean CLAY with sand and gravel (CL): tan, moist					
Dish ID	ST-117	Moist Soil + Dish (g)	206.06	Mass of Air-Dried Soil (g)		76.87
Dish Mass (g)	128.05	Dry Soil + Dish (g)	204.28	Corrected Dry Mass (g)		75.12
				Composite Correction		5

Time (min)	Hydro. Reading	Temperature (°C)	Effective Depth	Diameter (mm)	% Passing	Combined % Passing
2	53.0	18.5	7.6	0.0269	63.3%	39.5%
5	47.0	18.5	8.6	0.0181	55.4%	34.5%
15	40.0	18.5	9.7	0.0111	46.1%	28.8%
30	36.0	18.5	10.4	0.0081	40.9%	25.5%
60	32.0	18.5	11.1	0.0059	35.6%	22.2%
90	31.0	18.0	11.2	0.0049	34.3%	21.4%
120	30.0	18.0	11.4	0.0042	32.9%	20.6%
240	26.0	18.0	12.0	0.0031	27.7%	17.3%
480	23.0	17.5	12.5	0.0023	23.7%	14.8%
1440	20.0	17.5	13.0	0.0013	19.8%	12.3%

Gradation Curve
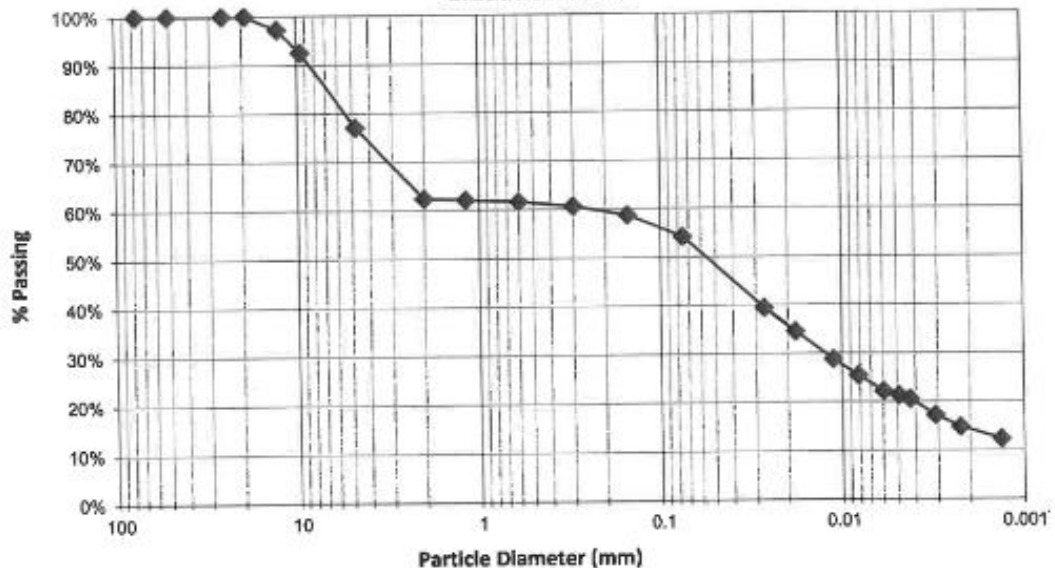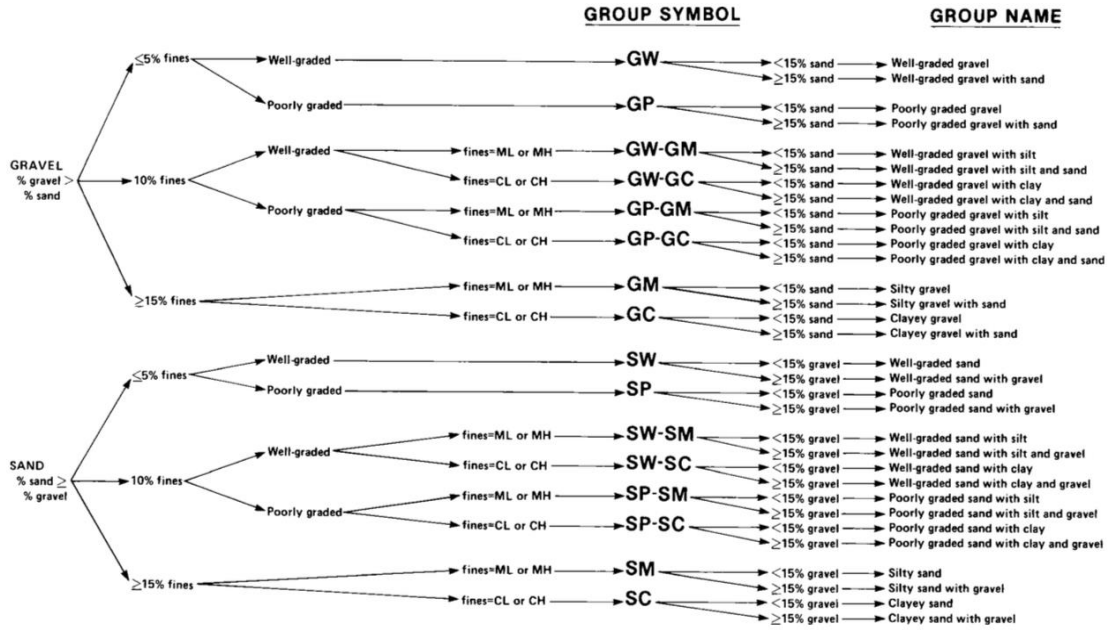
Figure A.1: Flow Chart for Identifying Coarse-Grained Soils (less than 50% fines)
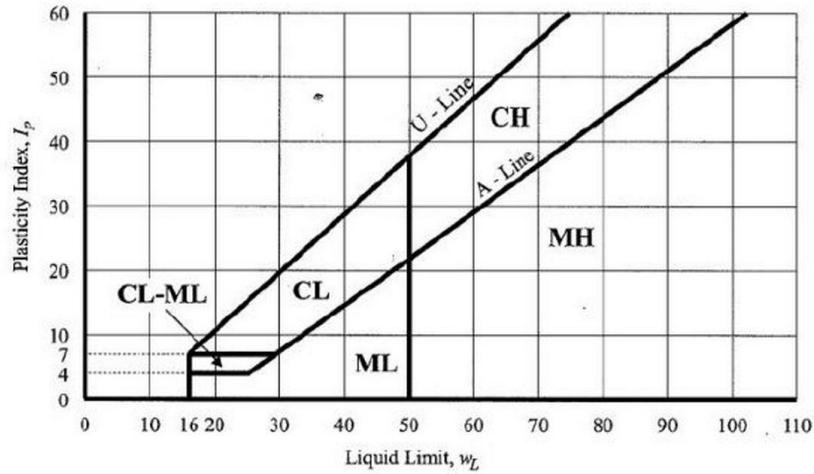
Figure A.2: Casagrande's Plasticity Chart

A.2.   Specific Gravity of Soil

SPECIFIC GRAVITY

Test performed in accordance to ASTM D854

Job #:	—	Job Name:	Quail Springs Cobb Wall Testing
Lab Job #:		Client:	

Boring #:	—	Sample #:	—	Depth (ft):	—
Soil Description:		Lean CLAY with sand and gravel (CL) tan, moist			

Initial Moisture Content (Moist Method)

Tare I.D.	213
Tare Mass, g	31.05
Wet Mass + Tare, g	57.55
Dry Mass + Tare, g	56.75
% Moisture	3.1%

Soil Type	Moist Mass, g with 250ml Pycnometer	Moist Mass, g, with 500 ml Pycnometer
SP, SP-SM	61.9	103.1
SP-SC, SM, SC	46.4	77.3
Silt or Clay	36.1	51.6

Note: Values in above table are generated from the reported %M and guidance from Table 2 of ASTM D854-06

Pycnomter and Test Data

Pycnometer I.D.	2
Calibrated Volume of Pycnometer, ml	498.96
Average Calibrated Mass of Dry Pycnomter, g	174.48
Mass of Pycnometer+Soil+Water, g	716.33
Test Temperature, C	20.8
Density of Water at Test Temp, g/ml	0.99804
Temperature Coefficient, K	0.99983

After Test Data

Tare I.D.	B13
Tare Mass, g	179.51
Dry Mass + Tare, g	248.49
Mass of Oven Dry Solids, g	68.98

Calculations

Mass of Pycnomter and Water at Test Temperature, g	672.46
Specific Gravity at Test Temperature	2.75
Specific Gravity at 20 Degrees C	2.75

Tested By:	GVP-LEB	Date:	11/29/18	Checked By:	ND

A.3. Liquid Limit, Plastic Limit, and Plasticity Index

DEPARTMENT OF CIVIL AND ENVIRONMENTAL ENGINEERING

Atterberg Limits Measurements

Test Method: ASTM D4318, D2487

Project Name	Quail Springs	Project No.	--
Tested By	LEB	Testing Date	4/23/2019

SPECIMEN ID AND CLASSIFICATION					
Boring No.	--	Sample No.	--	Depth (ft)	--
Soil Description	Cobb material,: Lean CLAY with sand and gravel (CL): yellowish brown				

LIQUID LIMIT				
Target Range of Blows	40-30	30-25	25-20	20-10
Actual Number of Blows	36	28	23	19
Dish ID	51	8	37	54
Mass of Dish (g)	30.67	30.59	30.82	30.61
Mass of Moist Soil + Dish (g)	40.61	48.05	38.91	40.84
Mass of Dry Soil + Dish (g)	38.06	43.51	36.76	38.18
Water Content	34.5%	35.1%	36.2%	35.1%

PLASTIC LIMIT		
Dish ID	67	83
Mass of Dish (g)	30.53	30.44
Mass of Moist Soil + Dish (g)	37.51	36.60
Mass of Dry Soil + Dish (g)	36.44	35.67
Water Content	18.1%	17.8%

SUMMARY	
Liquid Limt	35
Plastic Limit	18
Plasticity Ind.	17

Flow Curve

Plasticity Chart
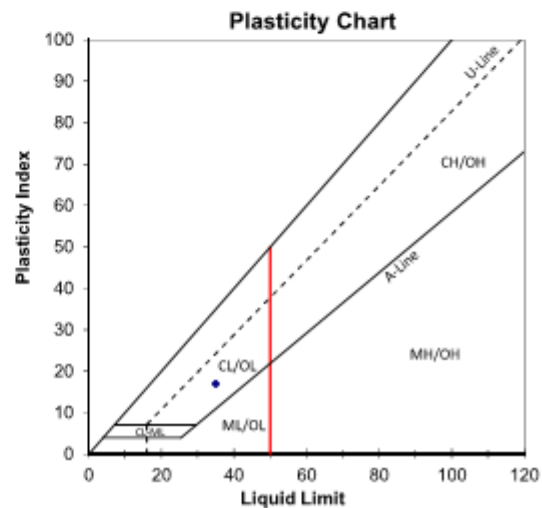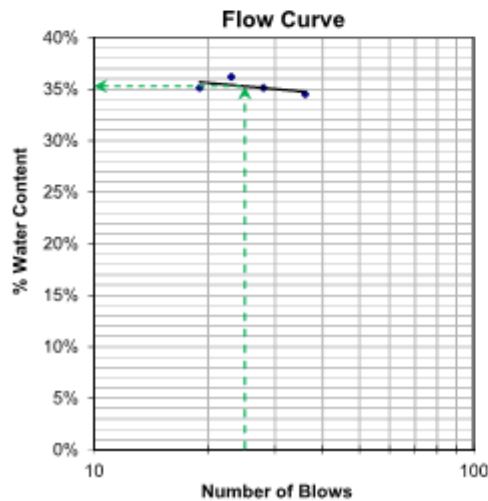
APPENDIX B. MODULUS OF RUPTURE TEST RESULTS

Block Properties	1-A	1-B	1-C	Average	St. Dev.
Bottom Middle Width (in)	7.25	7.38	7.11	7.25	0.14
Middle Height (in)	7.37	7.27	7.34	7.33	0.05
Area (in^2)	53.433	53.653	52.187	53.09	0.79
Length (in)	19.75	19.88	19.75	19.79	0.08
Mass (lb)	66.9	65.3	64.26	65.49	1.33
I (in^4)	241.8573	236.3080	234.3023	237.49	3.91
MOR Tests					
Date Tested	4/16/2019	4/17/2019	4/17/2019		
Support Span (in)	16	16	16	16	0
P_{max} (lb)	756	568	456	593.333	151.60
Distance from center (in)	1	1	1		
M_{rupt} (lb in)	2646	1988	1596	2076.67	530.59
f_r (psi)	40.3151	30.5803	24.9990	31.9648	7.7514
Δ_{max} from LVDT A (in)	0.02445	0.02962	0.03033	0.02813	0.00321
Δ_{max} from LVDT B (in)	0.07805	0.02868	0.02921	0.04531	0.02836
Comments:	Crack formed 1" off from center	Other method for MOR Test performed	Higher amounts of straw, but not most.		
	"LVDT in B" side crushed straw, so reading	Accidentally applied 300lbs prior to test.	Crack formed 0.5" off on close side		
		Crack formed 1" off from center	Crack formed 1" off on far side and shot out to 3"		

Block Properties	2-A	2-B	2-C	Average	St. Dev.
Bottom Middle Width (in)	7.11	7.03	-	7.07	0.06
Middle Height (in)	7.28	7.23	-	7.26	0.04
Area (in^2)	51.761	50.827	-	51.29	0.66
Length (in)	20	19.88	-	19.94	0.08
Mass (lb)	66.08	66.1	-	66.09	0.01
I (in^4)	228.6033	221.4058	-	225.00	5.09
MOR Tests					
Date Tested	4/17/2019	4/17/2019	-		
Support Span (in)	16	16	-	16	0
P_{max} (lb)	394	587	-	490.5	136.4716
Distance from center (in)	0.75	2	-		
M_{rupt} (lb in)	1428.25	1761	-	1594.625	235.2898
f_r (psi)	22.7417	28.7527	-	25.74721	4.250414
Δ_{max} from LVDT 1 (in)	0.00807	0.01855	-	0.01331	0.00741
Δ_{max} from LVDT 2 (in)	0.06233	0.11308	-	0.08771	0.03588
Comments:	Prior to test, big crack down the middle Crack formed 0.75" from center Rotation failure? LVDT readings were very off Lots of straw	Prior to test, little cracks were present on front side Crack formed 2" from center Lots of straw	*Not here*		

Block Properties	3-A	3-B	3-C	Average	St. Dev.
Bottom Middle Width (in)	7.32	7.38	7.26	7.32	0.06
Middle Height (in)	6.98	7.16	7.3	7.15	0.16
Area (in^2)	51.094	52.841	52.998	52.31	1.06
Length (in)	20	20.06	19.75	19.94	0.16
Mass (lb)	64.32	63.3	62.24	63.29	1.04
I (in^4)	207.4417	225.7429	235.3553	222.85	14.18
MOR Tests					
Date Tested	4/17/2019	4/17/2019	4/17/2019		
Support Span (in)	16	16	16	16	0
P_{max} (lb)	712	513	666	630.333	104.184
Distance from center (in)	3	0	0		
M_{rupt} (lb in)	1780	2052	2664	2165.33	452.766
f_r (psi)	29.9467	32.5421	41.3146	34.6011	5.95706
Δ_{max} from LVDT 1 (in)	0.06102	0.03411	0.05679	0.05064	0.01447
Δ_{max} from LVDT 2 (in)	0.05773	0.03899	0.05520	0.05064	0.01017
Comments:	Crack formed 3" off from the center	Other method for MOR Test performed	Big chunks on the bottom missing Higher on one side than the other		

Block Properties	4-A	4-B	4-C	Average	St. Dev.
Bottom Middle Width (in)	7.58	7.08	7.14	7.27	0.27
Middle Height (in)	6.96	6.94	6.72	6.87	0.13
Area (in^2)	52.757	49.135	47.981	49.96	2.49
Length (in)	20.13	20.13	20.25	20.17	0.07
Mass (lb)	-	65.6	63.6	64.60	1.41
I (in^4)	212.9687	197.2107	180.5613	196.91	16.21
MOR Tests					
Date Tested	4/11/2019	4/17/2019	4/17/2019		
Support Span (in)	16	16	16	16	0
P_{max} (lb)	534	635	606	591.667	52.0032
Distance from center (in)	0	0.5	1		
M_{rupt} (lb in)	2136	2381.25	2121	2212.75	146.118
f_r (psi)	34.9032	41.8990	39.4689	38.757	3.55185
Δ_{max} from LVDT 1 (in)	N/A	0.04549	0.04746	0.04647	0.00139
Δ_{max} from LVDT 2 (in)	N/A	0.04388	0.04809	0.04598	0.00297
Comments:		Other method for MOR Test performed	Crack formed 1" off from center		
		Prior to test, there were cracks on the top in middle	The top of block was wavy (different heights)		
		Crack formed 0.5" off from the center			

Block Properties	5-A	5-B	5-C	Average	St. Dev.
Bottom Middle Width (in)	7.46	7.33	7.33	7.37	0.08
Middle Height (in)	7.51	7.15	6.99	7.22	0.27
Area (in^2)	56.025	52.410	51.237	53.22	2.50
Length (in)	20	20.38	20.125	20.17	0.19
Mass (lb)	29.49 kg	65.38	64.12	64.75	0.89
I (in^4)	263.3161	223.2754	208.6192	231.74	28.31
MOR Tests					
Date Tested	4/16/2019	4/17/2019	4/17/2019		
Support Span (in)	16	16	16	16	0
P_{max} (lb)	684	491	555	576.667	98.3073
Distance from center (in)	1	2.5	0.5		
M_{rupt} (lb in)	2394	1350.25	2081.25	1941.83	535.66
f_r (psi)	34.1395	21.6197	34.8672	30.2088	7.44727
Δ_{max} from LVDT 1 (in)	0.03403	0.04325	0.01685	0.03138	0.01340
Δ_{max} from LVDT 2 (in)	0.04274	0.03672	0.02172	0.03373	0.01082
Comments:	Crack formed 1" off from center	Other method for MOR Test performed	Crack followed the path of straw		
		Crack formed 2.5" off from center	0.5" off on close side. 2" off on far side.		

Block Properties	6-A	6-B	6-C	Average	St. Dev.
Bottom Middle Width (in)	7.12	7.79	7.27	7.39	0.35
Middle Height (in)	6.92	6.16	6.64	6.57	0.38
Area (in^2)	49.270	47.986	48.273	48.51	0.67
Length (in)	19.88	21.13	20.56	20.52	0.63
Mass (lb)	66.38	65.2	66.88	66.15	0.86
I (in^4)	196.6152	151.7394	177.3607	175.24	22.51
MOR Tests					
Date Tested	4/17/2019	4/16/2019	4/16/2019		
Support Span (in)	16	16	16	16	0
P_{max} (lb)	206	685	556	482.333	247.851
Distance from center (in)	2	2.5	1.75		
M_{rupt} (lb in)	618	1883.75	1737.5	1413.08	692.434
f_r (psi)	10.8755	38.2363	32.5241	27.212	14.4332
Δ_{max} from LVDT 1 (in)	0.08900	0.03307	0.02375	0.04861	0.03529
Δ_{max} from LVDT 2 (in)	0.08567	0.03505	0.02787	0.04953	0.03150
Comments:	Prior to tests, cracks on the top in middle / Crack formed 2" from center	Crack formed 2.5" off from center	Crack formed 1.75" off from center		

Test Wall 5: Monolithic adobe, reinforced with straw, 6" x 6 gauge welded wire mesh, and posts of paired 2" drill stem

Reinforced Monolithic Adobe Test Walls for Full-Scale In-plane Tests with Cal Poly San Luis Obispo Summer / Fall 2018

Oasis Design

Plans

A101